Comprehensive modeling of Spinal Muscular Atrophy in *Drosophila melanogaster*

Ashlyn M. Spring[1]*, Amanda C. Raimer[1,2], Christine D. Hamilton[1],

Michela J. Schillinger[4], and A. Gregory Matera[1,2,3,4,5]

[1]Integrative Program in Biological and Genome Sciences, [2]Curriculum in Genetics and Molecular Biology, [3]Lineberger Comprehensive Cancer Center, [4]Department of Biology, [5]Department of Genetics, University of North Carolina, Chapel Hill, NC, 27599 USA

Abbreviated title: Spinal Muscular Atrophy in the Fly

*Address correspondence to: Dr. Ashlyn Spring
UNC SPIRE Program
University of North Carolina
250 Bell Tower Dr.
Chapel Hill, NC 27599-7100

Comprehensive modeling of Spinal Muscular Atrophy in *Drosophila melanogaster*

Abstract

Spinal muscular atrophy (SMA) is a common neurodegenerative disorder that affects motor neurons, primarily in young children. SMA is caused by loss-of-function mutations in the *Survival Motor Neuron 1 (SMN1)* gene and a corresponding reduction in SMN protein levels. SMN functions in the assembly of spliceosomal RNPs and is well conserved in many model systems including mouse, zebrafish, fruit fly, nematode, and fission yeast. Work in *Drosophila melanogaster* has focused on molecular and cellular functions of SMN, primarily using null alleles or strong hypomorphs. A systematic analysis of SMA-related phenotypes over a range of *Smn* alleles has not been performed in the fly. This has led to debate over the validity of *Drosophila* as a proper model for SMA. We therefore examined fourteen fly lines expressing single SMA patient-derived SMN missense mutations for defects in both the larval and adult stages. Animals were evaluated on the basis of organismal viability and longevity, locomotor function, neuromuscular junction structure and development, muscle health, and immune system function. In all cases, we observed phenotypes consistent with those found in human SMA patients. Severity of these defects is variable, and forms a broad spectrum across the fourteen lines examined. We assert that these fly lines constitute an effective model for SMA, recapitulating the full range of phenotypic severity observed in human SMA patients.

Significance Statement

Spinal Muscular Atrophy (SMA) is a neuromuscular disorder resulting from loss-of-function mutations in *survival motor neuron 1* (*SMN1*). Disease severity forms a broad spectrum in SMA patients ranging from onset *in utero* to adulthood. This spectrum has proven difficult to reproduce in mammalian systems, including mouse, which typically model either severe or mild forms of SMA, missing intermediate forms. Here, we use *Drosophila melanogaster* to analyze an allelic series of SMA-causing missense mutations and systematically assess SMA-related phenotypes. We found strong concordance between human and *Drosophila* phenotypes across a wide spectrum of severity and evidence of evolutionarily conserved roles for SMN in immune regulation and neuromuscular health. These findings validate the fruitfly as an effective, comprehensive model for SMA.

Introduction

Spinal Muscular Atrophy (SMA) is a neurodegenerative disease that primarily affects motor neurons in the anterior horn of the spinal cord and is a leading genetic cause of death among infants (Pearn, 1980). Symptoms involve muscle weakness that progressively worsens to the point of paralysis. The diaphragm becomes involved in later stages, leading to difficulty breathing and persistent respiratory infection that is a typical cause of death (Crawford, 2017). Although motor neurons are dramatically impacted, other tissues including the musculature, cardiovascular system, liver, pancreas, gastrointestinal tract, and immune system are also affected (Perez-Garcia *et al.*, 2017). SMA has a broad range of severity; symptomatic onset can occur *in utero* in the most severe cases or in adulthood in the least severe. This spectrum has been subdivided into different "types" of SMA (Darras and Finkel, 2017; Talbot and Tizzano, 2017) based on age of onset: Type 0 (*in utero*), Type 1 (first 6 months), Type 2 (7 to 18 months), Type 3 (childhood onset after 18 months), and Type 4 (adult onset).

SMA is most commonly caused by reduced levels of the Survival Motor Neuron (SMN) protein which in humans is encoded by two genes, *SMN1* and *SMN2* (Lefebvre *et al.*, 1995). SMN is ubiquitously expressed and canonically functions in assembly of spliceosomal snRNPs (Matera *et al.*, 2007; Matera and Wang, 2014; Gruss *et al.*, 2017). SMN is also reported to have other functions related to RNA trafficking, translation, endocytosis, cytoskeletal maintenance, and cellular signaling (Raimer *et al.*, 2017; Singh *et al.*, 2017; Chaytow *et al.*, 2018; Price *et al.*, 2018). The manner and degree to which these putative splicing-independent functions of SMN contribute to SMA pathogenesis is an area of ongoing research.

There is currently one FDA-approved SMA treatment: an antisense oligonucleotide (ASO) called nusinersen that increases SMN protein production from *SMN2* (Shorrock *et al.*, 2018). This therapeutic strategy prevents motor neuron dysfunction if treatment begins before or soon after symptomatic onset (Finkel *et al.*, 2017). In later-stage patients, ASO therapy halts

degeneration but does not restore lost function (Mercuri *et al.*, 2018). Thus, later-stage patients remain at high risk of complication and death.

The approved method of ASO delivery treats only the central nervous system, and while this is sufficient to prevent motor neuron dysfunction and early death, it appears likely that secondary symptoms will arise with age in peripheral systems of ASO treated patients (Hua *et al.*, 2015; Bowerman *et al.*, 2017). Therefore, there is an emerging need for SMA models that can be rapidly adapted to new research challenges. In this vein, *Drosophila melanogaster* is a useful model. Advantages of the fly include: low cost, rapid generation time, high quality genetic tools, well characterized organ systems and cellular pathways. Most important in the context of SMA, *Drosophila* has a single *Smn* gene that is conserved both at the level of protein sequence (Chan *et al.*, 2003) and molecular function (Rajendra *et al.*, 2007).

To date, work in the fly has focused primarily on assessing the effects of strong *Smn* depletion on organismal development (Rajendra *et al.*, 2007; Shpargel *et al.*, 2009) or larval synapses and muscles (Chan *et al.*, 2003; Chang *et al.*, 2008; Aquilina and Cauchi, 2018). This work has provided evidence that SMN's functions are conserved. However, in the fly and other model organisms, including mouse, there are few effective models for intermediate forms of SMA (Burghes *et al.*, 2017; O'Hern *et al.*, 2017). Nearly all of the models are severe and involve developmental delays or arrests that complicate analysis, including transcriptomic profiling of pre-mRNA splicing changes and neuromuscular development and function (Winkler *et al.*, 2005; McWhorter *et al.*, 2008; Hammond *et al.*, 2010; Garcia *et al.*, 2013; Garcia *et al.*, 2016).

Here, we present a set of fourteen SMA models that cover the full spectrum of SMA severity and, in many cases, circumvent problems of developmental delay. In these models, symptomatic onset occurs anywhere from early development to adulthood, suggesting that the system effectively models all SMA Types. The larval stages appear particularly useful for examining pre- and early-onset SMA, as we observe reduced locomotor function in the absence of synaptic or muscular defects. Conversely, the adult stage is best suited for modeling late-

onset SMA, as we observed reduced lifespan and locomotor deficits at different times post-eclosion. Similar to human patients, loss of motor function in adult flies is progressive and displays early involvement/affectation of posterior limbs relative to anterior ones. Additionally, we identified altered immune activity in our models. Based on these results, we propose that this system is useful for the study of classical neuromuscular phenotypes as well as peripheral aspects of SMA.

Materials and Methods

Fly lines and husbandry

Patient mutation lines, Smn^{X7}, Smn^{D}, *Da-Gal4*, "C15" driver line: *elav(C155)-Gal4; Sca-Gal4; BG57-Gal4*. From Bloomington: *TRiP.JF02057* (Smn-RNAi #1, Stock #26288), *TRiP.HMC03832* (Smn-RNAi #2, Stock #55158)

To generate lines expressing *Smn* missense mutations, Smn^{X7}/TM6B-GFP virgin females were crossed to Smn^{X7}, Smn^{TG}/TM6B-GFP males at 25°C. To reduce stress from overpopulation and/or competition from heterozygous siblings, crosses were performed on molasses plates with yeast paste and GFP negative, Smn^{X7}, Smn^{TG}/Smn^{X7} larvae were sorted into vials containing molasses fly food during the second instar larval stage. Sorted larvae were raised at 25°C until the desired developmental stage was reached.

Experiments involving *UAS-Smn-RNAi* expression were carried out at 29°C to maximize expression from the Gal4/UAS system and, therefore, the degree of *Smn* knockdown. The one exception to this is the adult locomotion assay performed on Da-Gal4/Smn-RNAi #2. Raising these animals at 29°C dramatically reduces viability and is incompatible with survival to the adult stage. To circumvent this and produce viable adults we instead raised all animals for this experiment at 25°C. To maintain consistency across experiments, we also use molasses plates with yeast paste and subsequent sorting for all *Smn-RNAi* experiments.

Viability Assays

To assess viability, we sorted 35-50 late second/early third instar larvae into vials containing standard molasses fly food and waited for them to complete development. After sufficient time had passed to allow for animals to complete development, we counted the total number of pupal cases in each vial and the number of empty pupal cases, which corresponds to the number of eclosed adults. We calculated % viability at both the pupal and adult stages by dividing these values by the number of initial larvae and then multiplying by 100 (pupal viability = (# total pupae/# initial larvae)*100, adult viability = (# empty pupal cases/# initial larvae)*100). Each vial is considered a biological replicate in respect to calculating averages and standard error. n-value represents the total number of larvae collected and assayed.

Determining the stage of pupal arrest involves an identical procedure to assessing pupal and adult viability with the exception of scoring the pupae. In this assay, we examined pupae under white light at 2X magnification and score them based on morphology as having arrested early in pupal development, in mid pupal development, late in pupal development, or as empty pupal cases (viable adults). These values were normalized to the total number of pupae.

Locomotion Assays

Larval Locomotion: One to five larvae at either the early third or wandering third instar stage were placed onto the center of the locomotion stage (a large molasses plate) at room temperature. The stage was then placed in a recording chamber to control light and reflection and provide support for video recording. Once all larvae were actively crawling, movement was recorded as video for at least 1 minute and 10 seconds on an iPhone 6S at minimum zoom. Two video recordings were taken for each set of larvae. Locomotion videos were transferred to a PC and converted to raw video avi files in ffmpeg. Video length was trimmed to exactly 60 seconds by removing the first 2 seconds and final additional second to 1) create videos of standard duration and 2) eliminate from the analyzed frames small movements caused by

starting and stopping the recording. Videos were opened and converted into binary images series in Fiji/ImageJ. The wrMTrck plugin for ImageJ was used to assess larvae size, larval body length, average speed of movement in pixels/second, and average speed normalized to larval size (body lengths/second).

Adult Locomotion: Adult flies of various ages were place in individual locomotion chambers consisting of 35 x 10 mm round tissue culture plates filled with 7.5 ml of clear agar to prevent movement in the Z-direction. Flies were given 5-6 hours to adjust to the new environment and then free moving walking behavior was recorded and analyzed in the same manner described for the larval locomotion assay.

Immunostaining

Third instar larvae were dissected in HL3 saline with the following components (and concentrations): NaCl (70 mM), KCl (5 mM), MgCl2 (10 mM), NaHCO3 (10 mM), sucrose (115 mM = 3.9%), trehalose (4.2 mM = 0.16%), HEPES (5.0 mM = 0.12%), and $CaCl_2$ (0.5 mM, unless otherwise indicated). Dissected samples were subsequently fixed with Bouin's fixative (Ricca Chemical Company, Arlington, TX) for 3 minutes. Fixed samples were washed in 1X PBST using standard procedures, and incubated in primary antibodies at 4°C for overnight. This was followed by additional washes and a two-hour incubation in secondary antibody at room temperature. Staining was performed using the following primary antibodies: mouse anti-Synapsin (3C11) 1:1000 (concentrated antibody, Developmental Studies Hybridoma Bank, University of Iowa - DSHB); rabbit anti-Dlg 1:30,000 (Budnik *et al.*, 1996). The following fluorophore-conjugated antibodies were also used: Alexa-488 goat anti-rabbit 1:5000 and Alexa-546 donkey anti-mouse 1:5000 (both from ThermoFischer/Invitrogen Life Technologies, Eugene OR), and Alexa-647 goat anti-HRP (Jackson ImmunoResearch Laboratoreis, Inc., West Grove, PA). Larval preparations were mounted in Antifade media and imaged on a Leica TCS SP5

AOBS UV/spectral confocal laser-scanning system mounted on an inverted DM IRE2 microscope.

Longevity Assay

To assess longevity, newly eclosed adult flies were collected daily into vials containing molasses agar food. Animals were kept with no greater than 10 animals total to avoid stress from crowding and transferred to fresh vials every 2-3 days to avoid death due to non-optimal food conditions. The number of adults was recorded at the time of collection and once each week following collection until all animals had expired. Animals that escaped or were injured/killed during transfer were excluded from analysis.

Collecting Partially Eclosed Adults

Animals were crossed and larvae collected as described above. As animals entered the pupal stage and began to either arrest and die or proceed through development. 2-3 days after pupal formation, viable pupae were transferred to an empty tissue culture dish for easy observation. Animals nearing the end of pupal development were observed for partial eclosion. Wild type flies eclose rapidly (within 1-10 seconds) under normal conditions. To be sure that Smn missense mutants were truly stuck in the partially eclosed state, we waited for 10 minutes following identification of potential partially-eclosed animals to see if they would complete eclosion. If they did not, we used fine forceps and microdissection scissors to remove partially eclosed animals from their pupal cases without damaging them. To control for the effects of possible stress during this assisted eclosion approach, we performed the same dissections/eclosion assist procedure on animals expressing wild type transgenic SMN that had completed pupal development but not yet eclosed.

Scoring Melanotic Masses

Wandering third instar larvae were removed form vials, washed briefly in a room temperature water bath, dried, and placed on an agar plate under white light and 2X magnification. When melanotic masses were identified in a larvae, both the size of the largest mass (size score) and the total number of masses (mass score) were qualitatively determined. Size scoring used the following criteria: small masses range in size from barely visible specks to smooth round dots with a diameter no more than 1/10th the width of the larva; medium masses range from anything larger than a small mass to those with a diameter up to 1/3 the larval width; large masses are any with a diameter greater than or equal to 1/3 the larval width. Larvae were manipulated to allow for observation of all sides/regions; observation was performed for at least 20 seconds in all cases.

Statistical analysis

All statistical analyses were performed using GraphPad Prism 7. For all data except longevity curves, p-values are from one-way ANOVA with a Dunnet correction for multiple comparisons. Statistical significance for longevity curves was determined by the Logrank/Mantel-Cox test. Details for the statistical analysis used in each figure panel are described in figure legends and/or shown in Table 1.

Results

To maximize the range of phenotypic severity examined in this study, *Drosophila* lines carrying transgenic insertions of fourteen different *Smn* alleles were examined, in addition to the Oregon R (OR) wild type lab strain. The inserted transgenes encode a wild type *Smn* allele (WT) along with thirteen alleles for non-synonymous *Smn* point mutations. Each mutation in this allelic series produces SMN protein with a single residue change homologous to those of human SMA

patients bearing small *SMN1* mutations (Table 2). In this work, we will refer to these transgenic lines by the amino acid substitution produced in the fly SMN protein (D20V, for example). A single copy of each missense mutation allele is expressed in an *Smn* null background (see Materials and Methods for full genotype). Thus the transgenic product is the sole form of SMN present in the animals after the maternal SMN contribution is fully depleted at the end of the second instar larval stage. For some Smn mutations, we have also generated stable, self-replicating lines with animals carrying the Smn transgene and two transheterozygous null mutations of the endogenous *Smn* gene. These flies lack maternally contributed wild type Smn at all stages of development.

It should be noted that expression of each of these transgenic *Smn* alleles is driven by the native 5' and 3' *Smn* flanking regions and inserted at an identical attP site on the third chromosome to standardize potential position effects. This genomic arrangement is reported to drive transgenic *Smn* expression at lower levels than the endogenous *Smn* gene (Praveen *et al.*, 2012). The Smn^{WT} transgenic line serves both as a control for this lower level of SMN expression and, in some assays described here, displays mild phenotypic changes relative to the wild type lab strain Oregon R (OR). All but one of these *Smn* missense lines has been previously reported and shown to cause variable degrees of developmental arrest or reduced viability (Praveen *et al.*, 2014). Here, we fully characterize these *Smn* alleles and report on an additional one. The new allele is based on a recently reported SMA mutation that produces a tyrosine to cysteine change at Y277 in the human (Y208 in *Drosophila*) SMN protein (Table 2).

Smn **missense mutations reduce viability across development**

We first sought to replicate the previously reported viability defects for each of these 14 lines at the pupal and adult stages (Fig. 1A). Consistent with previously published observations, our experiments produced a broad range of viability phenotypes. The most severe phenotype is full developmental arrest at the 2nd to 3rd instar transition, which was observed for the G206S,

M194R, and Y203C alleles. Animals carrying any of the other eleven *Smn* alleles reach pupation at moderate to normal levels, and all but one of them (V72G) produce viable adults to some degree (Fig 1A). The adult viability defects form a continuum that encompasses phenotypes from complete lethality (V72G) to nearly normal levels of viability (D20V and WT). This continuum is reminiscent of the spectrum of disease severity seen in SMA patients, indicating that this set of missense mutations has the potential to model a broad range of SMA Types.

A majority of these *Smn* alleles arrest during the pupal stage of development. To further explore this phenotype, we examined the timing of death during pupariation for each allele (Fig 1B,C). The pupal cases of developing *Drosophila* are transparent, so approximate staging can be performed visually using intact animals (Fig 1C). We observed arrest and death both early and late during pupal development for animals carrying all alleles except V72G, which causes arrest very shortly after pupariation (Fig 1B,C). Very few animals of any line arrested during the middle stages of pupation. Higher frequencies of arrest early in pupal development were observed for alleles that produce fewer viable adults.

Given the large number of individual genotypes described here, we organized these *Smn* alleles into four phenotypic classes based on gross viability phenotypes. Class I is the most severe, causing larval-stage arrest, and is comprised of G206S, M194R, and Y203C. Class II is comprised of the five most severe alleles that reach pupation: V72G, F70S, Y107C, G210V, and Y208C. A smal fraction (2-11%) of animals carrying Class II alleles eclose as adults. Class III alleles are more moderately affected, with ecolsion frequencies ranging from 20-45%. This class includes the T205I, G210C, I93F, and G73R alleles. Class IV includes the WT and D20V alleles, which are the least affected, displaying a moderate 20-30% decrease in adult viability relative to the Oregon R strain. Throughout this manuscript, data for the *Smn* alleles are arranged in order of severity, and the color scheme for each Class is maintained for ease of reference.

Smn missense mutations support viability when wild type SMN protein is completely absent

In combination with previous observations, the range of severities observed in our viability assays suggests that most *Smn* missense mutations retain at least partial function. This conclusion is complicated by the presence of maternally contributed SMN that is present during embryonic and early larval development. We therefore attempted to generate stable fly lines expressing only *Smn* missense mutations. To do this, we sought to generated flies carrying two different *Smn* null alleles (Smn^{X7} and Smn^{D}) as well as one copy of each transgenic *Smn* allele (Smn^{TG}) for Class III and Class IV alleles. In all cases, adults of the desired genotype (Smn^{TG}, Smn^{X7}/Smn^{D}) were viable and sufficiently fertile to produce self-sustaining stocks. In later generations, animals in these stocks animals can carry either one or two copies of the Smn transgene and completely lack wild type SMN in all stages of development.

Having created these stocks, we assessed the functionality of *Smn* missense mutations by measuring developmental viability (Fig 2). We found that, in all cases, expression of Class III and Class IV mutations is sufficient for robust pupal viability (Fig 2A) and adult viability ranging from the moderate to wild type levels (Fig 2B). This result definitively demonstrates that *Smn* missense mutations are functional in the absence of any wild type SMN protein.

Smn missense mutations cause defects in larval locomotion but not NMJ structure.

Manipulations that strongly reduce SMN levels are known to cause larval locomotion defects. It is not clear, however, if the moderate reduction of SMN function modeled by *Smn* missense alleles has the same functional impact as reduction of wild type SMN. To address this, we performed larval locomotion assays on all lines at the early third instar stage (72 hours post-egg lay) and in wandering third instar larvae for the eleven lines that reach this stage (Fig 3).

Larvae from all lines display reduced locomotion relative to Oregon R at the early third instar stage with the exception of G73R (Fig 3A,B). All three Class I alleles show a further

decrease in crawling speed relative to the wild type transgenic line, as do the G210C, G210V, F70S, and Y107C lines. The rest of the mutant lines display no significant difference from the wild type transgenic control, suggesting that the mildly hypomorphic nature of these alleles is driving their locomotor defects (Fig 3A,B).

By the wandering third instar stage, all surviving lines exhibit locomotion defects. The Class IV alleles show a mild but statistically significant reduction in crawling speed relative to the Oregon R wild type train (Fig 3D). These two Class IV *Smn* alleles (WT and D20V) are not significantly different from one another, whereas all Class II and three alleles show a significant reduction in locomotion both relative to OR and the WT transgenic lines (Fig 3D,E). These differences are not due to overall changes in larval size, as this measure is unchanged in the wandering third instar larvae carrying transgenic *Smn* alleles (Fig 3F) and is controlled for within the analysis, by measuring locomotion in terms of body lengths per second (BLPS).

Given these locomotor deficits and previous reports of reduced NMJ size in the case of strong loss of SMN, we next immunostained and counted boutons at the muscle 6/7 NMJ in abdominal segment A2 for all lines that reach the wandering third instar stage. Surprisingly, we did not observe a dramatic change in bouton number for any of these alleles. All lines showed a slight but non-significant decrease in bouton number relative to Oregon R, with the exception of the I93F allele, which does reach statistical significance (Fig 4 A,B). These findings suggest that the locomotion defects observed in these larvae are likely due to functional changes in motor neurons or in other upstream central neurons such as interneurons. We also assessed the area of muscle 6/7 in segment A2 to look for signs of muscle degeneration. At the wandering third instar, we observed no changes in muscle area for any *Smn* allele (Fig 4C). This indicates that the body wall muscles are not actively experiencing atrophy and that these larvae are in the early stages of symptomatic onset.

RNAi-mediated *Smn* knockdown phenocopies *Smn* missense alleles

We next sought to assess potential tissue-specific roles of SMN in the observed phenotypes. To address this question, we used the *Gal4/UAS* system to drive two different constructs that produce shRNAs targeting RNAi-based knockdown of *Smn* under control of a *UAS* enhancer element (Perkins *et al.*, 2015). These lines are *Smn-RNAi*^{JF02057} and *Smn-RNAi*^{HMC03832} and are referred to here as Smn-RNAi #1 and Smn-RNAi #2, respectively. Expression of these *UAS-RNAi* constructs is driven either ubiquitously with *Da-Gal4* (*Daughterless*) or concurrently in both neurons and muscles using the 'C15' driver line (Brusich *et al.*, 2015), which contains three Gal4 constructs: two pan-neuronal drivers, *elav(C155)-Gal4* and *Scaberous-Gal4,* and one muscle specific driver, *BG57-Gal4*. Crossing the C15 driver with the Smn-RNAi responder lines allows us to simultaneously deplete SMN in both muscles and neurons, the two cell types most closely linked to SMA pathology.

We first used these RNAi lines to asses pupal and adult viability (Fig 5A,B). Similar to the findings with the *Smn* allelic series, both ubiquitous and neuromuscular *Smn* knockdown caused a significant reduction in viability (Fig 5A). Ubiquitous knockdown causes an effect comparable to that of the V72G lines, strongly reducing pupal lethality and displaying complete lethality at the adult stage. In contrast, neuromuscular knockdown of *Smn* phenocopies the moderate Class III alleles, displaying fairly normal pupal viability and a moderate decline in adult viability (Fig 5A). These data suggest that neuronal and muscle tissues contribute to the viability defects observed following ubiquitous *Smn* knockdown and in animals ubiquitously expressing mutant *Smn* alleles.

We also examined locomotion in the context of *Smn* knockdown. Both ubiquitous and neuromuscular knockdown of *Smn* negatively impacted larval locomotion (Fig 5C). In the context of ubiquitous knockdown, the presence of the *Gal4* element alone did not impact the baseline locomotor phenotype. In contrast, *Gal4* expression in neuromuscular tissues from the C15 line caused a significant increase in crawling speed relative to the OR control (Fig 5C).

Relative to this increase, expressing Smn-RNAi using the C15 driver line caused a significant decrease in locomotor speed (Fig 5C). A similar decrease in larval velocity was also observed in the context of ubiquitous *Smn* knockdown. Specifically, ubiquitous knockdown with Smn-RNA #1 causes a significant reduction in crawling speed (Fig 5C). Unlike the lines expressing *Smn* missense alleles, ubiquitous knockdown also caused a significant reduction in the size of the muscle 6/7 neuromuscular junction relative to the Oregon R wild type strain (Fig 4A).

Overall, examination of SMA-related phenotypes in larvae reveals a spectrum of severities in the context of developmental viability and reveals a moderate reduction in locomotor behavior. However, we did not observe changes to larval NMJ structure or muscle size (Fig 4). This is likely due to the relatively mild to intermediate nature of the *Smn* mutations examined here, the effects of maternally contributed SMN, and the short duration of the larval stages. In the context of our SMA models, there is likely not enough time for degenerative phenotypes to manifest in the larval stages. Therefore, to examine potential progressive degenerative phenotypes, we turned to the adult stages.

***Smn* missense mutations and neuromuscular knockdown reduce adult longevity**

Ten lines expressing transgenic *Smn* alleles produce viable adults to varying degrees (Fig 1A). We first used these adults to assess longevity, with the expectation that *Smn* mutations would shorten lifespan. Animals of the control Oregon R strain lived as long as 12 weeks, with 90% of individuals dying by 11 weeks of age (Fig 6A-D, gray line). The line expressing transgenic *Smn* (WT) is moderately hypomorphic and shows a signficant decrease in longevity as compared to OR, with increased death occurring by week 4 in the case of WT (Fig 6A-C).

All other lines expressing missense *Smn* alleles show a further, statistically significant reduction in longevity relative to WT (Fig 6A-D). The Class IV mutation, D20V, begins to display impaired longevity relative to WT beginning at week 7 and 90% of animals carrying this mutation are deceased by 7.6 weeks of age (Fig 6A, D). The decrease in longevity is more pronounced

for the Class III mutations (G73R (Fig 6A), I93F, T205I, and G210C (Fig 6B), which begin to deviate from WT between 3-6 weeks of age (Fig 6B,C) and reach 90% death by 6-7 weeks (Fig 6D). The Class II mutations (G210V, Y208C, Y107C, and F70S) are the most severely impacted, with significant death occurring as early as the first week of life (Fig 6C,D).

We next sought to assess the possibility that the reduced longevity observed for missense *Smn* lines is related to neuromuscular health. To do so, we again turned to RNAi-mediated *Smn* knockdown in the neuromusculature. The C15 Gal4 driver line was used to express each of the two *UAS-Smn-RNAi* constructs in adult flies. To maximize shRNA expression, flies were raised at 29°C which increases the efficiency of the yeast-derived Gal4 protein as a transcriptional activator. Under these conditions, the OR strain displays reduced longevity/lifespan relative to other controls such as the Gal4 alone (C15/+) or the Smn-RNAi constructs alone (Smn-RNAi/+) (Fig 7A-C). Neuromuscular expression of Smn-RNAi #1 moderately affected longevity relative to the C15/+ and Smn-RNAi #1/+ controls, although they outlived the OR controls (Fig 7A, C). The effect with Smn-RNAi #2 was much stronger, with all animals expiring within the first week of life (Fig 7B,C). These findings suggest that the longevity defects observed in the case of missense *Smn* alleles is due, at least in part, to loss of *SMN* function in neurons and muscles.

Smn missense alleles and neuromuscular knockdown reduce adult locomotion

To more directly assess neuromuscular function in adult flies we performed an adult locomotion assay on free moving animals in a circular chamber with restricted vertical space to prevent flight. Flies were collected and assayed within 24-36 hours after eclosing (Fig 8) and after aging for 5 and 6 weeks in certain cases (Fig 9). At one day of age, both Class IV alleles (WT and D20V) and two of the Class III alleles (G73R and I93F) showed robust locomotor behavior. These animals display walking speeds that are slightly faster than that of the Oregon R wild type strain and are not significantly different from one another (Fig 8A, B). The remaining Class III

alleles (T205I and G210C) showed a moderate but significant decrease relative to the WT transgenic line. The Class II alleles showed robust and significant impairment in their locomotor behavior relative to both WT and Oregon R (Fig 8A,B).

Similar effects were observed for both ubiquitous and neuromuscular knockdown of *Smn* (Fig 8C-E). As was the case for larval locomotion, Gal4 expression alone leads to increased adult walking speeds. Relative to Gal4 controls, ubiquitous *Smn* knockdown using the Smn-RNAi #2 line produces a moderate but significant reduction in adult walking speed (Fig 8C). Neuromuscular *Smn* knockdown with Smn-RNAi #2 also reduces walking speed relative to both the C15 Gal4 line control and the Oregon R wild type strain. In this case the reduction was dramatic, as many animals remained essentially stationary during the assay (Fig 8D,E). This finding suggests that the locomotor defects observed in animals expressing mutant *Smn* alleles are due to dysfunction in neuronal and/or muscular tissues. Collectively, these data suggest that the adult stage can be used to model SMA-related phenotypes in the fly.

Class IV and Class III Smn missense alleles are models for late-onset SMA

Three missense *Smn* alleles (D20V, G73R, and I93F) displayed robust adult locomotor behavior at one day of age (Fig 8A,B). In contrast, these lines also show reduced longevity as adults (Fig 6), mildly reduced viability (Fig 1), and impaired locomotion as larvae (Fig 3). These results indicated that these mutations have a relatively mild impact on *SMN* function and led us to hypothesize that these lines might be useful for modeling late-onset SMA. To test this, we aged flies carrying each of these three mutations as well as animals expressing the WT *Smn* transgene and assayed adult walking behavior weekly (Fig 9A). By 5 weeks of age, flies expressing the D20V, G73R, or I93F mutant *Smn* all showed a significant reduction in walking speed relative to the animals expressing the WT *Smn* transgene (Fig 9A,B,D). This decline persisted into the 6th week of life (Fig 9A,C,D), but could not be effectively assessed beyond that point due to the limited number of animals that survive into the 7th week of life. Interestingly, this

decline in locomotor function occurs 1-2 weeks prior to the time at which most of these flies began to die in the longevity assay (Fig 6), consistent with a causative link between the locomotor deficit and death. Based on this late-onset locomotor dysfunction, we conclude that these lines represent the first models of late-onset SMA in fly.

Smn mutant alleles and knockdown cause progressive loss of motor function

We analyzed the more severe Class II lines for progressive loss of motor function. We noticed that certain animals failed to fully eclose from their pupal cases and ultimately died (Fig 10A,B). This phenotype was most prevalent for the intermediate Class III mutations, and was less frequently observed for the more severe Class II mutations. This inverse relationship between allele severity and incidence of partial eclosion is likely due to the fact that most animals carrying Class II mutations arrest prior to reaching these later stages of development (Fig 1A,B).

We hypothesized that partial eclosion occurs in part due to severe muscle weakness in a subset of animals expressing missense *Smn*. To test this, we selected two lines, Y208C and G210V, which are both phenotypically severe in other assays yet produce enough late-stage animals to make analysis feasible. We monitored pupae for these lines on an hourly basis to identify animals that were unable to escape their pupal cases. Once identified, forceps and microdissection scissors were used to help these animals complete eclosion ("assisted eclosion"). We first put these animals through the adult locomotion assay and found that they had very low walking speeds and in many cases did not move at all (Fig 10C). Additionally, the lifespan of these animals was dramatically reduced relative to both wild type and normally eclosing adults of the same genotype (Fig 10D, Fig 6C,D). All animals examined died within 6 days of assisted eclosion (Fig 10D). To ensure that our assisted eclosion techniques were not harming the animals or impairing their locomotor function or survival, we performed the same procedure on Smn^{WT} (WT) pharate adults. Analysis of lifespan and locomotor function of these

animals was included for control purposes. As expected, the WT animals were unaffected by the manipulation (Fig 10C,D).

Similar phenotypes were also observed for animals expressing neuromuscular knockdown of *Smn* with Smn-RNAi #2. These animals are able to eclose without assistance but display severe adult locomotor dysfunction in the adult walking assay on day after eclosion (Fig 8F,G). Neuromuscular *Smn* knockdown also leads to dramatically reduced lifespan almost identical to that seen for the partially eclosed animals examined, with all animals dying within 6 days of life (Fig 10A).

Although walking speed was near zero for all of the mutant lines discussed above, qualitative observation suggested that these animals were not fully paralyzed and retained some degree of motor control over their legs at the time of assisted eclosion. To determine if motor control deteriorated over time in these animals, we turned to qualitative observation and scoring of locomotor function in a manner similar to clinical analysis of human patients. For 10-30 individual animals per genotype, we monitored leg function under the stereoscope for 1-2 minutes and assigned a leg score for each of the three leg pairs. Scoring was performed on a scale of 0 to 10, with complete paralysis scored as 0 and normal function scored as 10. Scoring was performed every 4-8 hours for the first 12 hours of life, followed by observation every 24 hours until death occurred. Using this method, we determined that partially eclosed flies expressing G210V and Y208C mutant *Smn* experience progressive loss of leg function over time (Fig 11A-C). Interestingly, individual leg pairs were differentially affected at the time of assisted eclosion. The most anterior pair initially presented with mild to moderate impairment, whereas the most posterior pair was more severely impaired. The function of all three leg pairs decreases over time, and the defects in the anterior and posterior limbs become more similar over time (Fig 11B,C). This is reminiscent of SMA disease progression in human patients who often develop muscle weakness in the legs prior to onset of in the arms.

Similar defects in leg function were observed upon examination of animals expressing Smn-RNAi #2 in neurons and muscles. Progressive loss of motor function was observed for all legs in aggregate (Fig 11D), and for individual leg pairs (Fig 11E,F). Additionally, we noted the same differential impact on individual leg pairs, with the anterior pair initially displaying much milder dysfunction than the most posterior pair (Fig 11E,F). None of these effects was observed for Oregon R controls reared and scored in the same manner (Fig 11D,E). Overall, the progressive loss of motor function and differential timing of affectation between posterior and anterior leg pairs suggests that these fly models of SMA are useful for modeling nuanced aspects of SMA onset and progression.

Smn missense alleles cause innate immune activation

Recently, defects in the development of immune cells and tissues have been reported in several mouse models of SMA (Deguise *et al.*, 2017; Khairallah *et al.*, 2017). Our examination of *Smn* missense mutations in the fly have also revealed role for SMN in immune tissues (Fig. 12). With the exception of an RNAi-mediated response to certain viruses (Wang *et al.*, 2006), *Drosophila melanogaster* does not have an adaptive immune response. However, it does possess a robust innate immune system. The innate immune response is mediated by macrophage-like cells, collectively called hemocytes. The molecular pathways and mechanisms that regulate hemocyte development and activity are conserved from fly to human and include Toll, TNF, and TGF-β signaling (Williams, 2007; Gold and Bruckner, 2015). When activated, hemocytes encapsulate invading particles and melanize in an attempt to sequester and kill the pathogen. This leads to the formation of melanin-containing granules in the hemolymph which are readily observed through the transparent body wall of the larva. These granules are commonly referred to as pseudotumors, melanotic tumors, and melanotic masses.

Melanotic masses usually form at an elevated frequency in response to pathogens or damaged and necrotic tissue. Here, we report that melanotic masses are present at elevated

levels in all lines expressing *Smn* missense mutations in the absence of a pathogen (Fig 12). To quantify this phenomenon, we scored both the size and number of melanotic masses in individual larvae for each *Smn* missense mutation line. All lines examined displayed a statically significant and robust increase in the presence of melanotic masses relative to the Oregon R control line (Fig 12A). The WT transgenic *Smn* line is the most mildly impacted and all lines expressing mutant forms of *Smn* have significantly higher frequency of melanotic masses relative to WT (Fig 12A). Size scoring (Fig 12B) and counts of the total number of melanotic masses per animal (Fig 12C) show similar trends to the overall incidence of masses. Class IV mutations are moderately impacted, whereas both Class III and Class II mutations cause robust immune activation and melanotic mass formation (Fig 12A-D). These observations suggest that the function of SMN in immune tissues is conserved from flies to mammals and that *Smn* mutations in the fly can be used to model peripheral defects of SMA in addition to the canonical SMA-related neuromuscular phenotypes.

Discussion

We carried out a systematic assessment of SMA-related phenotypes at multiple developmental stages in flies expressing one of thirteen patient-derived *Smn* missense mutations. Additionally, we examined the effects of ubiquitous or neuromuscular-specific *Smn* knockdown. We identified viability defects resulting from developmental arrest for all alleles. These defects ranged from 100% arrest at the beginning of the third larval instar (M194R, G206S, and Y203C) to ~30% arrest by the pharate adult stage (D20V), with a spectrum of severities in between. In larvae, we were able to identify locomotion deficits for all lines except D20V. These behavioral changes were largely independent of structural defects at the NMJ or muscle. Similar effects were observed upon ubiquitous and neuromuscular Smn knockdown. Collectively, these observations support continued use of the larval stages to model the pre- and early-onset phases of SMA.

In adults, we observed reduced lifespan and locomotor defects in the context of *Smn* missense mutations as well as neuromuscular *Smn* knockdown. In most cases, locomotor defects were present from day 1 post-eclosion. For three mutations (D20V, G73R, and I93F), we did not observe locomotion defects at this early age and instead documented onset of defects at 5 weeks of age. Additionally, careful analysis of the most severely impacted adults – those unable to free themselves from their pupal cases – revealed phenotypes that mimic symptomatic hallmarks of SMA. First, we observed a difference in the timing of onset of severe locomotor dysfunction in anterior vs. posterior leg pairs. Two missense mutations (G210V and Y208C) and neuromuscular *Smn* knockdown (C15 x Smn-RNAi #2) caused the posterior legs to be strongly impaired at the time of eclosion whereas the anterior legs were either mildly affected or normal. We also observed rapid and progressive loss of motor function in these animals. Upon eclosion, many animals were able walk in a slow, uncoordinated manner. This functionality was quickly lost and progressed to complete paralysis and death within a week. These symptoms closely mimic those seen in SMA patients, who often present with difficulty in the legs prior to involvement of the arms and display rapid, progressive loss of motor function following the onset of symptoms. These data illustrate the potential of the adult fly to model milder forms of SMA.

In addition to analyzing phenotypes classically related to SMA, we also assessed these fly models for evidence of peripheral defects that are being reported in human patients and/or mouse models. This class of defects is important in the context of currently-approved SMA therapies, which effectively corrects the primary symptoms related to motor neuron dysfunction and early death, but leaves peripheral tissues untreated. The most readily observable peripheral phenotype in our models is formation of melanotic masses, an indicator of a hyper-activated immune system. SMN is known to play a role in immune system development and inflammatory signaling in several mouse models. Our findings suggest that immune regulation is a conserved

function for SMN and demonstrate that peripheral defects can be modeled in fly in addition to traditional neuromuscular phenotypes.

***Modeling SMA in Drosophila* larvae**

As mentioned above, previous studies of SMA in the fly have almost exclusively focused on examining molecular and cellular functions of *Smn* in the larval stages. Our analysis reveals larval locomotor defects but no sign of neuronal or muscle degeneration. Reduced NMJ and muscle size have been previously reported in the context of *Smn* null larvae (Chang 08; Imlach 12). These defects do not appear to represent a true degenerative phenotype but are likely an effect of developmental delay and arrest at the organismal level. NMJ and muscle size increase is proportional to whole animal growth. *Smn* null larvae are much smaller overall relative to age-matched controls (Shpargel 09; Praveen 14). As such, their muscles and NMJs are expected to be non-specifically reduced in size as well. Relative to *Smn* null animals, most of the missense mutations examined here were found to improve developmental viability. These data suggest that SMA missense mutations successfully restore partial SMN function.

There may also be tissue-specific developmental defects in the muscles and motor neurons of these animals. However, such defects are difficult to separate from the effects of overall developmental arrest. Tissue-specific rescue of *Smn* mutants and RNAi-mediated *Smn* knockdown in larvae have been useful tools in addressing this issue. For example, reducing *SMN* levels in motor neurons is sufficient to trigger developmental defects at the NMJ, characterized by a reduction in the stereotyped number of boutons at larval NMJs (Dimitriadi 10; Sen 11). In agreement with these results, we also observed reduced NMJ bouton number and locomotor defects upon ubiquitous *Smn* knockdown (Fig 6). Notably, under these RNAi conditions, we did not observe widespread developmental arrest in the larval stage. These results suggest that, as is seen in mouse models (PMID: 18603534; PMID: 2157233), reducing SMN levels leads to developmental defects at NMJs.

Whereas defects in development of NMJs and muscles have been observed in larvae, no overt evidence of motor neuron degeneration or muscle atrophy has been documented. Lack of degeneration in larvae is likely due to several factors. First, a functionally significant maternal contribution of SMN is present in the 1st and 2nd larval instar stages (Praveen 12; 14). Second, the entirety of larval development takes place over 5 days and the 3rd instar stage, during which maternal SMN is depleted, lasts only 2 days. This is a relatively short time frame in the cellular context of neurodegeneration and may be too narrow a window to allow phenotypes to develop. In the case of *Smn* missense models, the combination of the partial functionality of the mutant proteins and the limited time window without maternally contributed SMN appears to be sufficient to prevent degeneration. The ability to track onset of locomotor deficits and study synaptic changes that occur prior to the onset of degenerative phenotypes will be important for our understanding of SMA onset and progression.

Modeling SMA in adult stage Drosophila

This study represents the first report of adult models of SMA in the fly, using either expression of patient-derived *Smn* missense mutations or concurrent knockdown of *Smn* in neurons and muscles. These models have a shortened lifespan and locomotor defects, with variable ages of onset. Additionally, analysis of pharate adult animals too weak to fully eclose without assistance revealed several striking similarities with human SMA patients. These animals initially display much stronger impairment of their posterior legs relative to the mildly affected anterior leg pair. These animals also display rapid and progressive loss of motor function that leads to death. These findings are similar to the observed disease progression in human SMA patients.

Another advantage of adult models is the separation between severe developmental complications and neuromuscular phenotypes. In typical cases, SMA patients appear healthy and normal at the time of birth with onset of impaired motor function occurring months or years after birth. Creating models that mimic this aspect of SMA has been difficult in the mouse, as

most genetic manipulations that are sufficient to produce neuromuscular phenotypes also cause animals to be small, underdeveloped, and severely affected at the time of birth (Monani ; Hsieh Li 2000). Pups for these models fail to grow significantly and die in the first weeks of life, reminiscent of Type 0 SMA in humans. Our Class III and IV fly models produce adults of normal size that appear otherwise healthy upon eclosion. These animals continue to mature as normal until they die between 1 and 7 weeks of life (control flies live for 12-13 weeks). Using animals that successfully progress through all developmental stages allows for separation of SMA phenotypes from gross developmental issues. This is important, as developmental arrest can independently affect mRNA processing and gene expression, nervous system development and growth, as well as many other phenotypes relevant to the study of SMA (Garcia 2013; 2016; carrel 2006;McWhorter 2008; Perez Garcia 2015). The ability to avoid these complications with genetic models that develop normally adds a valuable tool to the field of SMA research.

Modeling intermediate forms of SMA.

Mouse models for late-onset SMA have been difficult to generate. Copy number changes in human *SMN2* transgenes or C>T mutation of the endogenous mouse *Smn* allele cause dramatic shifts in phenotype from mild and largely unaffected to very severe with onset of symptoms *in utero* and death between 4-14 days after birth (Monani ; Hsieh Li 2000). Addition of partially functional SMN-producing genes, such as *SMNΔ7* or *SMN2* leads to a similar bifurcation of phenotypes (Le 2005 PMID: 15703193; Osborne et al. 2012). Depending on the gene dose, mice are either strongly affected at birth or completely rescued throughout life. This binary relationship between SMN dosage and phenotype in mice has led to a dearth of robust mouse models of intermediate SMA. Consequently, the processes that precede onset of neuromuscular dysfunction and motor neuron death have been difficult to study in murine systems.

In the fly, we observe a more continuous range of phenotypic severity across many assays in the context of hypomorphic SMN levels and partial function. The mildest *Smn* missense mutations we assessed (D20V, G73R, and I93F) are phenotypically wild type at the time of eclosion. By 5 weeks of age, however, flies carrying these mutations begin to show locomotor dysfunction and expire after 1-3 additional weeks of life. Based on these observations, we assert that these three *Smn* missense mutations model moderate, later-onset Type III and IV SMA. These models will be a useful tool in examining the full range of SMA disease progression from pre-onset changes to organismal death in a single biological context.

SMN missense mutations are partially functional in the absence of wild type SMN protein

Together with previous work (Praveen, Garcia, Gray), the data presented here demonstrate that many SMN missense mutations retain partial function. As discussed above, the maternal contribution of SMN complicates this interpretation in early larval stages. By the start of the third instar larval stage, however, the maternal contribution is fully depleted and complete lack of SMN rapidly leads to developmental arrest and death. In our models, transgenic *Smn* is expressed from the native promotor throughout the life of the organism. In this context, we observe survival to differential degrees and developmental stages for each *Smn* missense mutations. For example, flies expressing the V72G mutation all arrest shortly after pupating, whereas those expressing the G210C mutation begin to arrest in pupal development, reaching adulthood at a frequency of ~20%. Animals expressing the D20V mutation arrest as late-stage pupae and reach adulthood at a frequency of ~70%. These findings demonstrate that *Smn* missense mutations specifically modify the null phenotype and are inconsistent with the notion that they extend viability due to secondary effects caused by non-specific stabilization of the maternal contribution.

Furthermore, we successfully generated stable, viable fly stocks that exclusively express certain missense alleles of *Smn* in an otherwise *Smn* null background (*Flag-Smn*^{TG},

Smn^{X7}/*Smn*^{D}). These animals are viable and fertile in the absence of any wild type SMN at any stage of their development, providing conclusive evidence that *Smn* missense mutations are at least partially functional in our system. Given the conservation of SMN protein structure from fly to human, we expect that this finding holds true in human patients as well. Our results are in direct contrast to of those of a recent report using the SMNΔ7 mouse model, claiming that two mild patient-derived missense mutations (D44V and T741I) are non-functional in the absence of full-length SMN (Iyer PMID: 29982416). This assertion is based on a single finding: that mice expressing only *SMN* missense mutations do not survive to birth. While this result clearly indicates that these two *SMN* missense mutations are not fully functional, it by no means rules out the possibility of partial function.

Smn null mice arrest at the blastula stage of embryonic development (Schrank *et al.*, 1997). Missense alleles that fully lack function would be expected to arrest at the same stage as the null allele. Unfortunately, neither this stage nor any other embryonic stage was assessed in the context of the D44V or T274I mutations to determine if *SMN* missense mutations partially rescue embryonic development (Iyer *et al.*, 2018). Notably, all of the human *SMN* missense alleles analyzed in the mouse to date have been expressed from randomly-integrated, variable copy number, cDNA-based transgenes (Gavrilina *et al.*, 2008; Workman *et al.*, 2009; Iyer *et al.*, 2018). Moreover, none of these studies uses a wild-type cDNA control, so it is difficult to compare the transgenic lines without the ability to control for expression levels, position effects, or secondary mutations caused by integration.

Indeed, transgenic rescue of embryonic lethality using human *SMN* constructs in the mouse is fraught with complication. Mice expressing two randomly-inserted cDNA copies of *SMN*Δ*7* die within 5 days of birth when crossed onto the FVB background (Monani *et al.*, 2000). However, this same *SMN*Δ*7* transgene completely fails to rescue embryonic lethality when crossed onto a C57/BL6 background (Gogliotti *et al.*, 2011; Osborne *et al.*, 2012; Meier *et al.*, 2018). Expressing one or two copies of human *SMN2* in an *Smn* null background is also

insufficient to rescue embryonic lethality in mouse (Osborne *et al.*, 2012). These results are in contrast to the effects of manipulating SMN expression from the endogenous mouse locus. Mice bearing a C>T mutation in exon 7 of the endogenous *Smn* gene (mimicking human *SMN2*) are fully viable and fertile (Gladman *et al.*, 2010; Hammond *et al.*, 2010). Further, these mice live a normal lifespan when the C>T allele is present in either the homozygous or hemizygous state, displaying mild adult-onset phenotypes (Gladman *et al.*, 2010). This incongruity suggests that expression of randomly-inserted human *SMN* cDNAs is suboptimal in the context of restoring mouse viability. In fact, there is no evidence that a wild-type human *SMN* cDNA transgene can rescue mouse viability, as such a line has yet to be reported. For all of these reasons, additional work is needed in this area.

Concordance between SMA severity and *Drosophila* phenotypes.

The missense mutations examined here impact residues in the SMN protein that are well conserved from fly to human. Thus, we expect that mutating these residues will cause similar changes in SMN protein function and/or stability in both species. An indirect approach to assess this expectation is to compare the severity of SMA-related phenotypes in flies and SMA type in humans. This analyisis is somewhat complicated by several factors.

First, the diagnosis and classification of SMA types has changed significantly over the 20 year period since the first *SMN1* missense mutations were reported. Thus, cross comparison of severity between patients diagnosed in different decades is imperfect. For example, a severe patient diagnosed with Type I SMA that was reported in the late 1990's might be diagnosed as a Type 0 patient in the 2010's. Similarly, a patient diagnosed as Type II two decades ago might be considered a Type III patient today.

Second, a major complicating factor is *SMN2* copy number. In several reports of missense mutations from the late 1990s, the *SMN2* copy number of the patient was neither assessed nor reported (Table 2). Given the strong influence that *SMN2* copy number has on

SMA severity, lack of this information prevents reasonable comparisons of human and fly SMA phenotypes. As mentioned above, genetic background is also known to modify SMA severity. Moreover, *SMN1* missense mutations are extremely rare and often reported in single patients or a pair of affected siblings whose disease severity is impacted by genetic background to an unknown degree.

From the perspective of the fly data, there are far fewer complicating genetic factors to consider. The fourteen Flag-tagged *Smn* lines described here were generated in a single genetic background, with a single copy of the transgene inserted at the identical chromosomal location. This approach allows for direct, reliable comparison of phenotypic severity between patient mutations in the fly. An important caveat is that fly development includes multiple body plans (larval vs adult) and stages of development (embryonic, larval, and pupal) prior to the adult stage and it is therefore difficult to directly compare to the relatively linear process of human development. For example, it is unclear how the onset of symptoms in larval stages compares to age of onset in human development. Due to this, phenotypic Class and SMA type are not expected to align in terms of the number-designation. However, we do expect to see a correlation between human SMA Type and *Drosophila* Class designations, with the most severe human mutations also being the most severe in fly and vice versa.

Indeed, the information in Table 3 reveals that in almost every case, the severity observed in the fly is well aligned with human SMA Type. The one exception is the I93F/I116F mutant. Given that this mutation has only been observed in a single human patient, it is difficult to determine whether this residue is not as functionally important for fly SMN as it is for human, or if confounding factors such as genetic background might enhance the SMA severity in a manner that is independent of *SMN1*.

In all other cases, we observe strong concordance between the phenotypic severity of fly and human. For example, the fly mutations Y203C and M194R cause the most severe phenotype in flies, phenocopying null alleles. The same is seen in human patients carrying

Y272C and M263R mutations, which also phenocopy the *SMN1* null state in causing Type 1 SMA in the presence of 1 or 2 copies of *SMN2*. On the other end of the spectrum, the D44V, G95R, and T274I mutations appear to *improve* the SMA Type in patients relative to the severity expected based on *SMN2* copy number. For example, humans hemizygous for both *SMN2* and $SMN1^{T274I}$ display a relatively mild, Type 2 phenotype. Flies expressing the corresponding mutations (D20V, G73R, and T205I) are also mildly affected, with G73R and D20V causing adult-onset of locomotor defects. Overall, when appropriately considering SMA Type and *SMN2* copy number, we conclude that SMN missense mutations modeled in the fly faithfully recapitulate the human phenotypes.

References

Aquilina B, and Cauchi RJ. (2018) Modelling motor neuron disease in fruit flies: Lessons from spinal muscular atrophy. J Neurosci Methods: in press.

Bowerman M, Becker CG, Yanez-Munoz RJ, Ning K, Wood MJA, Gillingwater TH, Talbot K, and Consortium USR. (2017) Therapeutic strategies for spinal muscular atrophy: SMN and beyond. Dis Model Mech 10: 943-954.

Brusich DJ, Spring AM, and Frank CA. (2015) A single-cross, RNA interference-based genetic tool for examining the long-term maintenance of homeostatic plasticity. Front Cell Neurosci 9: 107.

Budnik V, Koh YH, Guan B, Hartmann B, Hough C, Woods D, and Gorczyca M. (1996) Regulation of synapse structure and function by the Drosophila tumor suppressor gene dlg. Neuron 17: 627-640.

Burghes AHM, DiDonato CJ, McGovern VL, and Arnold WD. (2017). Mammalian Models of Spinal Muscular Atrophy. In: Spinal Muscular Atrophy: Disease Mechanisms and Therapy (Sumner CJ, Paushkin S, and Ko CP, eds.): Academic Press, 241-260.

Chan YB, Miguel-Aliaga I, Franks C, Thomas N, Trulzsch B, Sattelle DB, Davies KE, and van den Heuvel M. (2003) Neuromuscular defects in a Drosophila survival motor neuron gene mutant. Hum Mol Genet 12: 1367-1376.

Chang HC, Dimlich DN, Yokokura T, Mukherjee A, Kankel MW, Sen A, Sridhar V, Fulga TA, Hart AC, Van Vactor D, and Artavanis-Tsakonas S. (2008) Modeling spinal muscular atrophy in Drosophila. PLoS One 3: e3209.

Chaytow H, Huang YT, Gillingwater TH, and Faller KME. (2018) The role of survival motor neuron protein (SMN) in protein homeostasis. Cell Mol Life Sci.

Clermont O, Burlet P, Benit P, Chanterau D, Saugier-Veber P, Munnich A, and Cusin V. (2004) Molecular analysis of SMA patients without homozygous SMN1 deletions using a new strategy for identification of SMN1 subtle mutations. Hum Mutat 24: 417-427.

Crawford TO. (2017). Standard of Care for Spinal Muscular Atrophy. In: Spinal Muscular Atrophy: Disease Mechanisms and Therapy (Sumner CJ, Paushkin S, and Ko CP, eds.): Academic Press, 43-62.

Cusco I, Barcelo MJ, del Rio E, Baiget M, and Tizzano EF. (2004) Detection of novel mutations in the SMN Tudor domain in type I SMA patients. Neurology 63: 146-149.

Darras BT, and Finkel RS. (2017). Natural History of Spinal Muscular Atrophy. In: Spinal Muscular Atrophy: Disease Mechanisms and Therapy (Sumner CJ, Paushkin S, and Ko CP, eds.): Academic Press, 399-421.

Deguise MO, De Repentigny Y, McFall E, Auclair N, Sad S, and Kothary R. (2017) Immune dysregulation may contribute to disease pathogenesis in spinal muscular atrophy mice. Hum Mol Genet 26: 801-819.

Finkel RS, et al. (2017) Nusinersen versus Sham Control in Infantile-Onset Spinal Muscular Atrophy. New Engl J Med 377: 1723-1732.

Garcia EL, Lu Z, Meers MP, Praveen K, and Matera AG. (2013) Developmental arrest of Drosophila survival motor neuron (Smn) mutants accounts for differences in expression of minor intron-containing genes. RNA 19: 1510-1516.

Garcia EL, Wen Y, Praveen K, and Matera AG. (2016) Transcriptomic comparison of Drosophila snRNP biogenesis mutants reveals mutant-specific changes in pre-mRNA processing: implications for spinal muscular atrophy. RNA 22: 1215-1227.

Gavrilina TO, McGovern VL, Workman E, Crawford TO, Gogliotti RG, DiDonato CJ, Monani UR, Morris GE, and Burghes AH. (2008) Neuronal SMN expression corrects spinal muscular atrophy in severe SMA mice while muscle-specific SMN expression has no phenotypic effect. Hum Mol Genet 17: 1063-1075.

Gladman JT, Bebee TW, Edwards C, Wang X, Sahenk Z, Rich MM, and Chandler DS. (2010) A humanized Smn gene containing the SMN2 nucleotide alteration in exon 7 mimics SMN2 splicing and the SMA disease phenotype. Hum Mol Genet 19: 4239-4252.

Gogliotti RG, Lutz C, Jorgensen M, Huebsch K, Koh S, and Didonato CJ. (2011) Characterization of a commonly used mouse model of SMA reveals increased seizure susceptibility and heightened fear response in FVB/N mice. Neurobiol Dis 43: 142-151.

Gold KS, and Bruckner K. (2015) Macrophages and cellular immunity in Drosophila melanogaster. Semin Immunol 27: 357-368.

Gruss OJ, Meduri R, Schilling M, and Fischer U. (2017) UsnRNP biogenesis: mechanisms and regulation. Chromosoma 126: 577-593.

Hammond SM, Gogliotti RG, Rao V, Beauvais A, Kothary R, and DiDonato CJ. (2010) Mouse survival motor neuron alleles that mimic SMN2 splicing and are inducible rescue embryonic lethality early in development but not late. PLoS One 5: e15887.

Hua Y, Liu YH, Sahashi K, Rigo F, Bennett CF, and Krainer AR. (2015) Motor neuron cell-nonautonomous rescue of spinal muscular atrophy phenotypes in mild and severe transgenic mouse models. Genes Dev 29: 288-297.

Iyer CC, Corlett KM, Massoni-Laporte A, Duque SI, Madabusi N, Tisdale S, McGovern VL, Le TT, Zaworski PG, David Arnold W, Pellizzoni L, and Burghes AHM. (2018) Mild SMN missense alleles are only functional in the presence of SMN2 in mammals. Hum Mol Genet.

Khairallah MT, Astroski J, Custer SK, Androphy EJ, Franklin CL, and Lorson CL. (2017) SMN deficiency negatively impacts red pulp macrophages and spleen development in mouse models of spinal muscular atrophy. Hum Mol Genet 26: 932-941.

Kotani T, Sutomo R, Sasongko TH, Sadewa AH, Gunadi, Minato T, Fujii E, Endo S, Lee MJ, Ayaki H, Harada Y, Matsuo M, and Nishio H. (2007) A novel mutation at the N-terminal of SMN Tudor domain inhibits its interaction with target proteins. J Neurol 254: 624-630.

Lefebvre S, Burglen L, Reboullet S, Clermont O, Burlet P, Viollet L, Benichou B, Cruaud C, Millasseau P, Zeviani M, and et al. (1995) Identification and characterization of a spinal muscular atrophy-determining gene. Cell 80: 155-165.

Matera AG, Terns RM, and Terns MP. (2007) Non-coding RNAs: lessons from the small nuclear and small nucleolar RNAs. Nat Rev Mol Cell Biol 8: 209-220.

Matera AG, and Wang Z. (2014) A day in the life of the spliceosome. Nat Rev Mol Cell Biol 15: 108-121.

McWhorter ML, Boon KL, Horan ES, Burghes AH, and Beattie CE. (2008) The SMN binding protein Gemin2 is not involved in motor axon outgrowth. Dev Neurobiol 68: 182-194.

Meier ID, Walker MP, and Matera AG. (2018) Gemin4 is an essential gene in mice, and its overexpression in human cells causes relocalization of the SMN complex to the nucleoplasm. Biol Open 7.

Mercuri E, et al. (2018) Nusinersen versus Sham Control in Later-Onset Spinal Muscular Atrophy. N Engl J Med 378: 625-635.

Monani UR, Sendtner M, Coovert DD, Parsons DW, Andreassi C, Le TT, Jablonka S, Schrank B, Rossoll W, Prior TW, Morris GE, and Burghes AH. (2000) The human centromeric survival motor neuron gene (SMN2) rescues embryonic lethality in Smn(-/-) mice and results in a mouse with spinal muscular atrophy. Hum Mol Genet 9: 333-339.

O'Hern P, Garcia EL, Hao LT, Hart AC, Matera AG, and Beattie CE. (2017). Nonmammalian Animal Models of Spinal Muscular Atrophy. In: Spinal Muscular Atrophy: Disease Mechanisms and Therapy (Sumner CJ, Paushkin S, and Ko CP, eds.): Academic Press, 221-239.

Osborne M, et al. (2012) Characterization of behavioral and neuromuscular junction phenotypes in a novel allelic series of SMA mouse models. Hum Mol Genet 21: 4431-4447.

Pearn J. (1980) Classification of spinal muscular atrophies. Lancet 1: 919-922.

Perez-Garcia MJ, Kong L, Sumner CJ, and Tizzano EF. (2017). Developmental Aspects and Pathological Findings in Spinal Muscular Atrophy. In: Spinal Muscular Atrophy: Disease Mechanisms and Therapy (Sumner CJ, Paushkin S, and Ko CP, eds.): Academic Press, 21-42.

Perkins LA, et al. (2015) The Transgenic RNAi Project at Harvard Medical School: Resources and Validation. Genetics 201: 843-852.

Praveen K, Wen Y, Gray KM, Noto JJ, Patlolla AR, Van Duyne GD, and Matera AG. (2014) SMA-causing missense mutations in survival motor neuron (Smn) display a wide range of phenotypes when modeled in Drosophila. PLoS Genet 10: e1004489.

Praveen K, Wen Y, and Matera AG. (2012) A Drosophila model of spinal muscular atrophy uncouples snRNP biogenesis functions of survival motor neuron from locomotion and viability defects. Cell Rep 1: 624-631.

Price PL, Morderer D, and Rossoll W. (2018) RNP Assembly Defects in Spinal Muscular Atrophy. Adv Neurobiol 20: 143-171.

Prior TW. (2007) Spinal muscular atrophy diagnostics. J Child Neurol 22: 952-956.

Raimer AC, Gray KM, and Matera AG. (2017) SMN - A chaperone for nuclear RNP social occasions? RNA Biol 14: 701-711.

Rajendra TK, Gonsalvez GB, Walker MP, Shpargel KB, Salz HK, and Matera AG. (2007) A Drosophila melanogaster model of spinal muscular atrophy reveals a function for SMN in striated muscle. J Cell Biol 176: 831-841.

Schrank B, Gotz R, Gunnersen JM, Ure JM, Toyka KV, Smith AG, and Sendtner M. (1997) Inactivation of the survival motor neuron gene, a candidate gene for human spinal muscular atrophy, leads to massive cell death in early mouse embryos. Proc Natl Acad Sci U S A 94: 9920-9925.

Shorrock HK, Gillingwater TH, and Groen EJN. (2018) Overview of Current Drugs and Molecules in Development for Spinal Muscular Atrophy Therapy. Drugs 78: 293-305.

Shpargel KB, Praveen K, Rajendra TK, and Matera AG. (2009) Gemin3 is an essential gene required for larval motor function and pupation in Drosophila. Mol Biol Cell 20: 90-101.

Singh RN, Howell MD, Ottesen EW, and Singh NN. (2017) Diverse role of survival motor neuron protein. Biochim Biophys Acta 1860: 299-315.

Skordis LA, Dunckley MG, Burglen L, Campbell L, Talbot K, Patel S, Melki J, Davies KE, Dubowitz V, and Muntoni F. (2001) Characterisation of novel point mutations in the survival motor neuron gene SMN, in three patients with SMA. Hum Genet 108: 356-357.

Sun Y, Grimmler M, Schwarzer V, Schoenen F, Fischer U, and Wirth B. (2005) Molecular and functional analysis of intragenic SMN1 mutations in patients with spinal muscular atrophy. Hum Mutat 25: 64-71.

Talbot K, Rodrigues NR, Ignatius J, Muntoni F, and Davies KE. (1997) Gene conversion at the SMN locus in autosomal recessive spinal muscular atrophy does not predict a mild phenotype. Neuromuscul Disord 7: 198-201.

Talbot K, and Tizzano EF. (2017) The clinical landscape for SMA in a new therapeutic era. Gene Ther 24: 529-533.

Wang CH, Papendick BD, Bruinsma P, and Day JK. (1998) Identification of a novel missense mutation of the SMN(T) gene in two siblings with spinal muscular atrophy. Neurogenetics 1: 273-276.

Wang XH, Aliyari R, Li WX, Li HW, Kim K, Carthew R, Atkinson P, and Ding SW. (2006) RNA interference directs innate immunity against viruses in adult Drosophila. Science 312: 452-454.

Williams MJ. (2007) Drosophila hemopoiesis and cellular immunity. J Immunol 178: 4711-4716.

Winkler C, Eggert C, Gradl D, Meister G, Giegerich M, Wedlich D, Laggerbauer B, and Fischer U. (2005) Reduced U snRNP assembly causes motor axon degeneration in an animal model for spinal muscular atrophy. Genes Dev 19: 2320-2330.

Wirth B, Herz M, Wetter A, Moskau S, Hahnen E, Rudnik-Schoneborn S, Wienker T, and Zerres K. (1999) Quantitative analysis of survival motor neuron copies: identification of subtle SMN1 mutations in patients with spinal muscular atrophy, genotype-phenotype correlation, and implications for genetic counseling. Am J Hum Genet 64: 1340-1356.

Workman E, Saieva L, Carrel TL, Crawford TO, Liu D, Lutz C, Beattie CE, Pellizzoni L, and Burghes AH. (2009) A SMN missense mutation complements SMN2 restoring snRNPs and rescuing SMA mice. Hum Mol Genet 18: 2215-2229.

Yamamoto T, et al. (2014) Intragenic mutations in SMN1 may contribute more significantly to clinical severity than SMN2 copy numbers in some spinal muscular atrophy (SMA) patients. Brain Dev 36: 914-920.

Legends

Figure 1. *Smn* missense mutations produce a spectrum of viability defects. A and B) Developmental viability of animals expressing *Smn* missense mutations at the pupal stage (A) and the adult stage (B) % Viability is the proportion of animals that survive to the pupal/adult stage relative to the number of larvae initially collected. **C)** Viability of animals carrying *Smn* missense mutations through pupal development. In the case, ns indicates a p-value of 0.99 and *** indicates a p-value of exactly 0.0001 **D)** Representative images of the pupal stages assessed in C. **Data:** Bars show average. Error bars show standard error. Data points represent biological replicates of 35-50 animals each, n-values (shown as numbers in parentheses next to genotypes) reflect the number of individual animals counted. n-values are the same for panels A-C. **Statistical analysis:** Values above the data are p-values vs WT from one-way ANOVA using the Dunnet correction for multiple comparisons. The p-values shown are multiplicity adjusted p-values. Underlining denotes values that are statistically significant.

Figure 2. *Smn* missense mutations are sufficient for viability in the absence of maternally contributed wild type SMN. A and B) Developmental viability at the pupal stage (A) the adult stage (B) stable lines expressing only *Smn* missense mutations with maternal contribution of WT Smn present. **Data:** Bars show average. Error bars show standard error. Data points

represent biological replicates of 50 animals each, n-values (shown in parentheses next to genotypes) reflect the number of individual animals counted. **Statistical analysis:** Values above the data are p-values vs WT from one-way ANOVA using the Dunnet correction for multiple comparisons. The p-values shown are multiplicity adjusted p-values. Underlining denotes values that are statistically significant.

Figure 3. *Smn* missense mutations or knockdown reduces larval locomotion. A) Larval crawling speed, measured in body lengths/second, in early third instar larvae. **B)** Representative traces for the data shown in A. **C)** Larval size for the same animals measured in the locomotion assay in A. **D)** Larval crawling speed, measured in body lengths per second, in wandering third instar larvae. **E)** Representative traces for the data shown in D. **F)** Larval size for the same animals measured in the locomotion assay in D. Data Bars show averages, points represent individual larvae, error bars represent standard error, n-values (# individual larvae) are show in parentheses adjacent to genotype on x-axis. Statistical significance was determined by ANOVA (ns = not significant, *p<0,05, ** p<0.01, ***p<0.001).

Figure 4. *Smn* missense mutations or knockdown has modest effects on neuromuscular junction (NMJ) structure. A) Bouton counts from the muscle 6/7 NMJ in wandering third instar larvae. **B)** Representative images for the data shown in A. Red marks Discs Large (Dlg), green marks synapsin (syn), and blue marks neuronal membranes. **C)** Muscle 6/7 combined area for the NMJs measured in A. **Data:** Bars show average. Error bars show standard error. Data points and n-values (shown in parentheses next to genotypes) reflect the number of individual neuromuscular junctions (A) or muscles (C) assayed. **Statistical analysis:** Values above the data are p-values vs WT from one-way ANOVA using the Dunnet correction for multiple comparisons. The p-values shown are multiplicity adjusted p-values. Underlining denotes values that are statistically significant.

Figure 5. Neuromuscular *Smn* knockdown reduces viability and larval locomotion. A and B) Developmental viability at the pupal stage (A) and adult stage (B) for animals expressing *Smn* missense mutations. % Viability is the proportion of animals the survive to the pupal/adult stage relative to the number of larvae initially collected. **C)** Larval crawling speed, measured in body lengths/second, in early third instar larvae. **Data:** Bars show average. Error bars show standard error. For A and B, data points represent biological replicates of 30-50 animals each, n-values (shown in parentheses next to genotypes) reflect the number of individual animals counted. For C, data points and n-values (shown in parentheses next to genotypes) reflect the number of individual animals assayed. **Statistical analysis:** Values above the data are p-values vs WT from one-way ANOVA using the Dunnet correction for multiple comparisons. The p-values shown are multiplicity adjusted p-values. Underlining denotes values that are statistically significant.

Figure 6. *Smn* missense mutations reduce lifespan A-C) Survival curves for adult flies expressing *Smn* missense mutations. Data is split into three graphs for visual clarity. Colors correspond to phenotypic Class. **D)** Lifespan measured as the age at which 10% of animals remain alive for each missense mutation. Shown next to genotypes, n-value (# of individual flies), p^1 (p-value as compared to OR, and p^2 (p-value as compared to WT). p-values were generate by Chi square analysis using the logrank rank/Mantel-Cox test.

Figure 7. Neuromuscular *Smn* knockdown reduces lifespan. A and B) Survival curves for adult flies expressing Smn-RNAi in all neurons and muscles. **C)** Lifespan measured as the age at which 10% of animals remain alive for each missense mutation. Shown next to genotypes, n-value (# of individual flies), p^1 (p-value as compared to OR, p^2 (p-value as compared to C15 x OR), and p^3 (p-value as compared to the respective Smn-RNAi/+). p-values were generate by Chi square analysis using the logrank rank/Mantel-Cox test.

Figure 8. *Smn* missense mutations or knockdown reduces free moving adult locomotion. A) Adult walking speed, measured in pixels/second, in adults one day after eclosion for animals expressing *Smn* missense mutations . **B)** Representative traces for the data shown in A. **C and D)** Adult waking speed, measured in pixels per second, in adults one day after eclosion for animals expressing *Smn-RNAi* either ubiquitously with the Da-Gal4 driver (C) or in both neurons and muscle using the C15 driver line (D). **E)** Representative traces for the data shown in D. **Data:** Bars show average. Error bars show standard error. Data points and n-values (shown in parentheses next to genotypes) reflect the number of individual animals assayed. **Statistical analysis:** Values above the data are p-values vs WT from one-way ANOVA using the Dunnet correction for multiple comparisons. The p-values shown are multiplicity adjusted p-values. Underlining denotes values that are statistically significant.

Figure 9. Animals expressing mild *Smn* missense mutations develop late-onset locomotor defects as adults. A) Adult walking speed, measured in pixels/second, in adults ranging from one day of age (0 weeks) through 6 weeks of age for animals expressing the WT transgene or the D20V, G73R, I93F *Smn* missense mutations. **B and C)** Adult walking speed (pixels/second) for the same genotypes shown in A at either 5 weeks or age (B) or 6 weeks of age (C). **D)** Representative traces for the data shown in B **E)** Representative traces for the data shown in C. **Data:** In A, points show averages in B and C, bars show average. Error bars show standard error in all cases. Data points and n-values (shown in parentheses next to genotypes) reflect the number of individual animals assayed. **Statistical analysis:** Values above the data are p-values vs WT from one-way ANOVA using the Dunnet correction for multiple comparisons. The p-values shown are multiplicity adjusted p-values. Underlining denotes values that are statistically significant. Stars shown in A correspond to exact p-values shown in B and C.

Figure 10. *Smn* missense mutants exhibit defect in eclosion. A) Percent of total larvae that complete pupal development but only partially eclose from their pupal case. **B)** Representative images of the partial eclosion phenotype quantified in A. **C)** Adult walking speed (pixels/second) for partially eclosed animals expressing the wild type *Smn* transgene or the Smn missense mutations Y208C or G210V. **D)** Survival curve for the same animals assayed in C. **E)** Survival curve for animals expressing neuromuscular *Smn* knockdown. **Data:** Bars show average. Error bars show standard error. Data points and n-values (shown in parentheses next to genotypes) reflect the number of individual animals assayed. **Statistical analysis:** For A and C, values above the data are p-values vs WT from one-way ANOVA using the Dunnet correction for multiple comparisons. The p-values shown are multiplicity adjusted p-values. Underlining denotes values that are statistically significant. For D and E, values next to each survival curve are p-values generated by Chi square analysis using the logrank rank/Mantel-Cox test.

Figure 11. Progressive loss of motor function is observed in the legs of partially eclosed *Smn* missense mutants and in animals expressing neuromuscular Smn knockdown. A Qualitative leg function scores (average or all three leg pairs) over time for partially eclosed animals expressing the wild type *Smn* transgene (n=11) or the Y208C (n=10) or G210V (n=7) *Smn* missense mutations. **B-D)** Qualitative leg function scores for each leg pair over time for same animals as in A. **E)** Qualitative leg function scores (average or all three leg pairs) over time for animals expressing neuromusuclar *Smn* knockdown. **F and G)** Qualitative leg function scores for each leg pair over time for same animals as in E.

Figure 12. The innate immune system is activated in *Smn* missense mutants. A-C) Melanotic mass data for wandering third instar larvae expressing Smn missense mutations. The data in each panel a different measure of the melanotic mass phenotypes of the same set of larvae. **A)** Percent of larvae assayed that had one or more observable melanotic mass. **B)**

Qualitative size scoring of the largest melanotic mass in each larvae. **C)** The average number of melanotic masses per animal. **D)** Representative images of melanotic masses in animals expressing *Smn* missense mutations. **Data:** Bars show average. Error bars show standard error. In A, data points represent biological replicates of 10 animals each and n-values (shown in parentheses next to genotpes) reflect the number of individual animas assyed. In C, data points and n-values reflect the number of individual animals assayed. **Statistical analysis:** Values above the data are p-values vs WT from one-way ANOVA using the Dunnet correction for multiple comparisons. The p-values shown are multiplicity adjusted p-values. Underlining denotes values that are statistically significant.

Table 1. Statistical Analyses. Statistical analysis was performed using GraphPad Prism 7 and includes corrections for multiple comparisons when appropriate.

Table 2. SMN missense mutation information from human patients and fly. When multiple SMA types and *SMN2* copy numbers are present, the order of the information for each criterion corresponds such that the first SMA type shown corresponds to the first *SMN2* copy number listed for a given mutation, etc.

Table 3. Alignment of phenotypic severity between humans fly. *Smn* missense mutations are shown in order of least severe to most severe based on fly genotypes with the corresponding information from human patients. To prevent potentially inaccurate comparisons, the four missense mutations with unknown *SMN2* copy number (Y107C, G206S, G210C, and G210V, shown in Table 2) have been excluded.

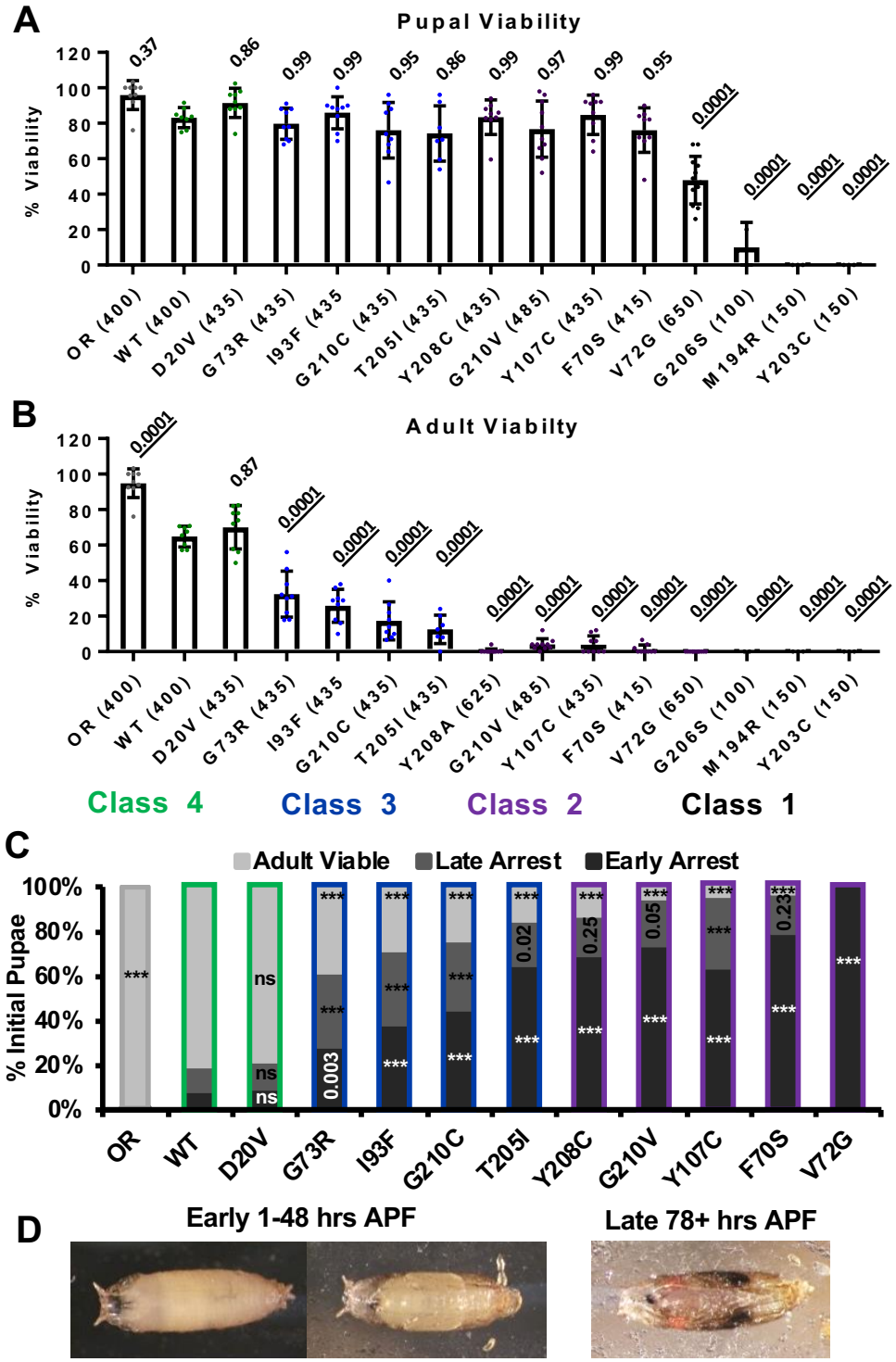

Figure 1. *Smn* missense mutations produce a spectrum of viability defects. A and B) Developmental viability of animals expressing *Smn* missense mutations at the pupal stage (A) and the adult stage (B) % Viability is the proportion of animals that survive to the pupal/adult stage relative to the number of larvae initially collected. **C)** Viability of animals carrying *Smn* missense mutations through pupal development. In the case, ns indicates a p-value of 0.99 and *** indicates a p-value of exactly 0.0001 **D)** Representative images of the pupal stages assessed in C. **Data:** Bars show average. Error bars show standard error. Data points represent biological replicates of 35-50 animals each, n-values (shown as numbers in parentheses next to genotypes) reflect the number of individual animals counted. n-values are the same for panels A-C. **Statistical analysis:** Values above the data are p-values vs WT from one-way ANOVA using the Dunnet correction for multiple comparisons. The p-values shown are multiplicity adjusted p-values. Underlining denotes values that are statistically significant.

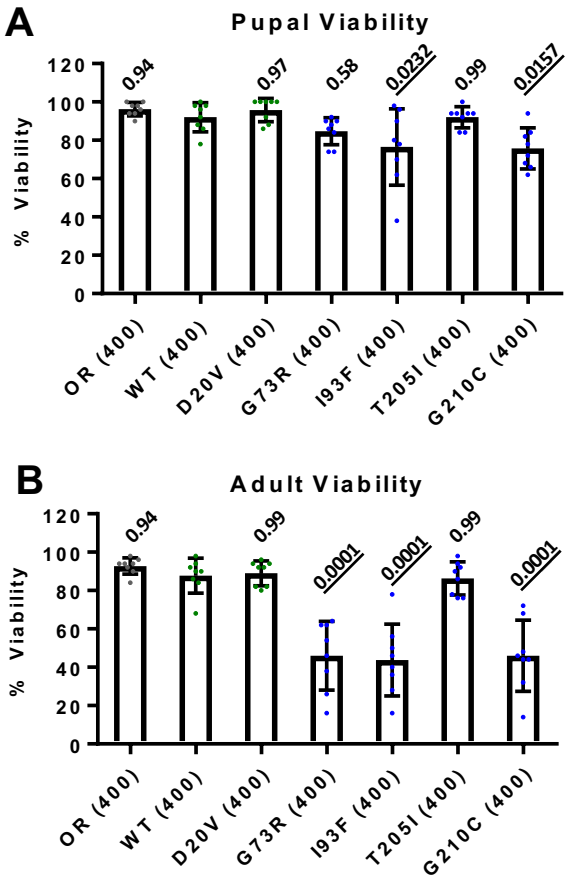

Figure 2. *Smn* missense mutations are sufficient for viability in the absence of maternally contributed wild type SMN. A and B) Developmental viability at the pupal stage (A) the adult stage (B) stable lines expressing only *Smn* missense mutations with maternal contribution of WT Smn present. **Data:** Bars show average. Error bars show standard error. Data points represent biological replicates of 50 animals each, n-values (shown in parentheses next to genotypes) reflect the number of individual animals counted. **Statistical analysis:** Values above the data are p-values vs WT from one-way ANOVA using the Dunnet correction for multiple comparisons. The p-values shown are multiplicity adjusted p-values. Underlining denotes values that are statistically significant.

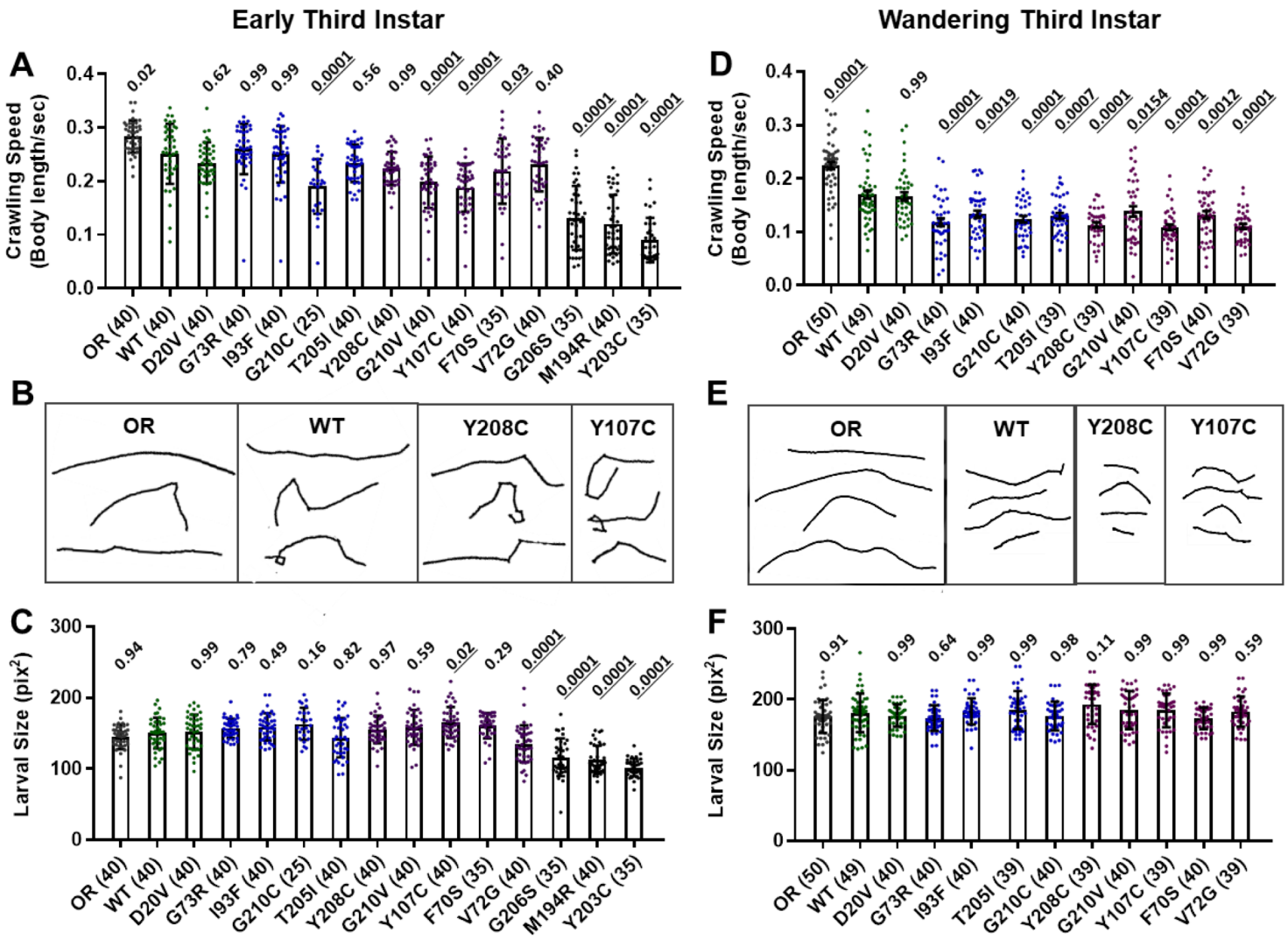

Figure 3. *Smn* missense mutations or knockdown reduces larval locomotion. A) Larval crawling speed, measured in body lengths/second, in early third instar larvae. **B)** Representative traces for the data shown in A. **C)** Larval size for the same animals measured in the locomotion assay in A. **D)** Larval crawling speed, measured in body lengths per second, in wandering third instar larvae. **E)** Representative traces for the data shown in D. **F)** Larval size for the same animals measured in the locomotion assay in D. Data Bars show averages, points represent individual larvae, error bars represent standard error, n-values (# individual larvae) are show in parentheses adjacent to genotype on x-axis. Statistical significance was determined by ANOVA (ns = not significant, *p<0,05, ** p<0.01, ***p<0.001)

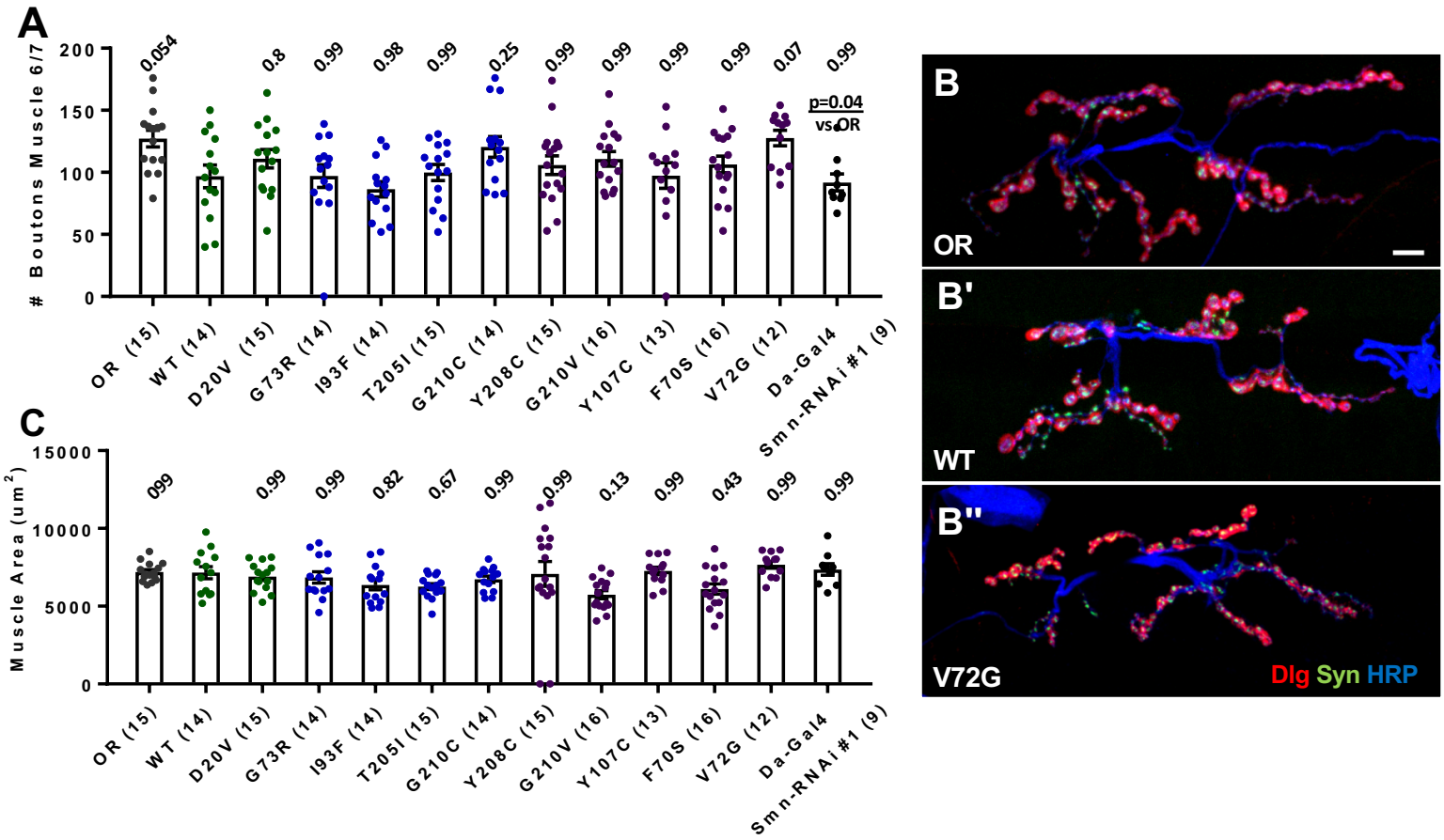

Figure 4. *Smn* missense mutations or knockdown has modest effects on neuromuscular junction (NMJ) structure. A) Bouton counts from the muscle 6/7 NMJ in wandering third instar larvae. **B)** Representative images for the data shown in A. Red marks Discs Large (Dlg), green marks synapsin (syn), and blue marks neuronal membranes. **C)** Muscle 6/7 combined area for the NMJs measured in A. **Data:** Bars show average. Error bars show standard error. Data points and n-values (shown in parentheses next to genotypes) reflect the number of individual neuromuscular junctions (A) or muscles (C) assayed. **Statistical analysis:** Values above the data are p-values vs WT from one-way ANOVA using the Dunnet correction for multiple comparisons. The p-values shown are multiplicity adjusted p-values. Underlining denotes values that are statistically significant.

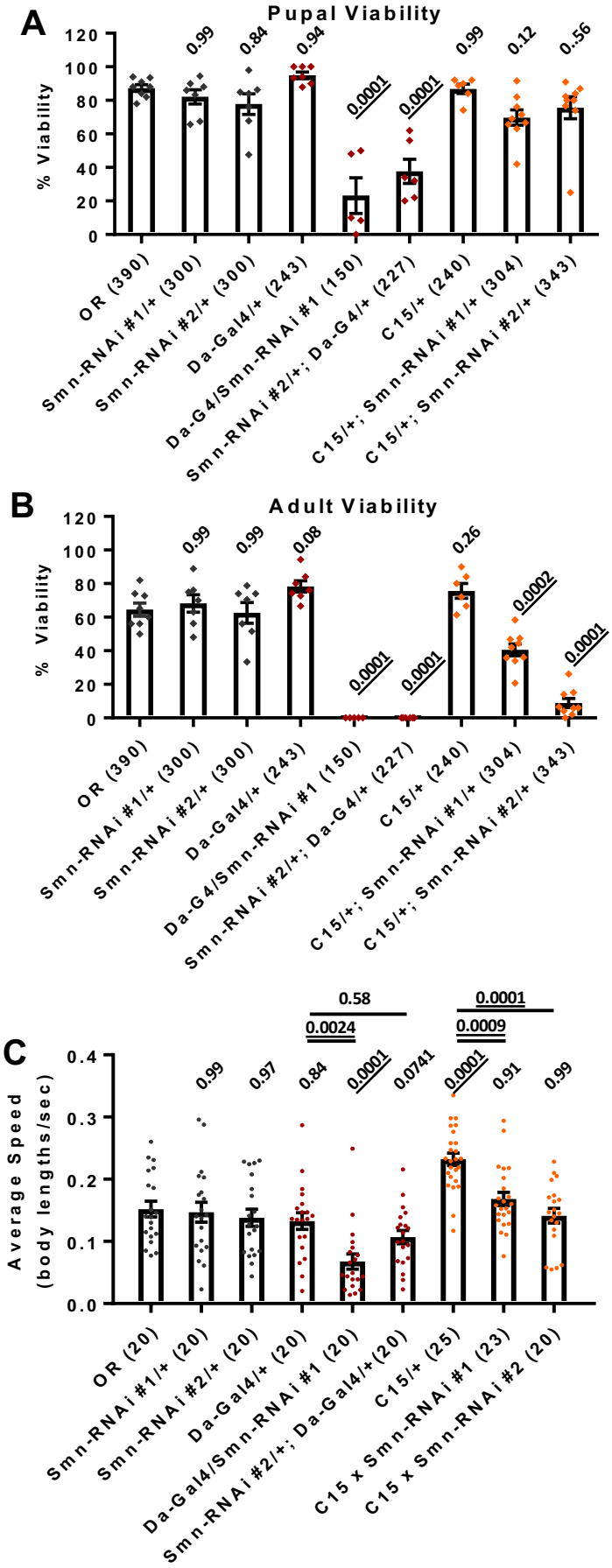

Figure 5. Neuromuscular *Smn* knockdown reduces viability and larval locomotion. A and B) Developmental viability at the pupal stage (A) and adult stage (B) for animals expressing *Smn* missense mutations. % Viability is the proportion of animals the survive to the pupal/adult stage relative to the number of larvae initially collected. **C)** Larval crawling speed, measured in body lengths/second, in early third instar larvae. **Data:** Bars show average. Error bars show standard error. For A and B, data points represent biological replicates of 30-50 animals each, n-values (shown in parentheses next to genotypes) reflect the number of individual animals counted. For C, data points and n-values (shown in parentheses next to genotypes) reflect the number of individual animals assayed. **Statistical analysis:** Values above the data are p-values vs WT from one-way ANOVA using the Dunnet correction for multiple comparisons. The p-values shown are multiplicity adjusted p-values. Underlining denotes values that are statistically significant.

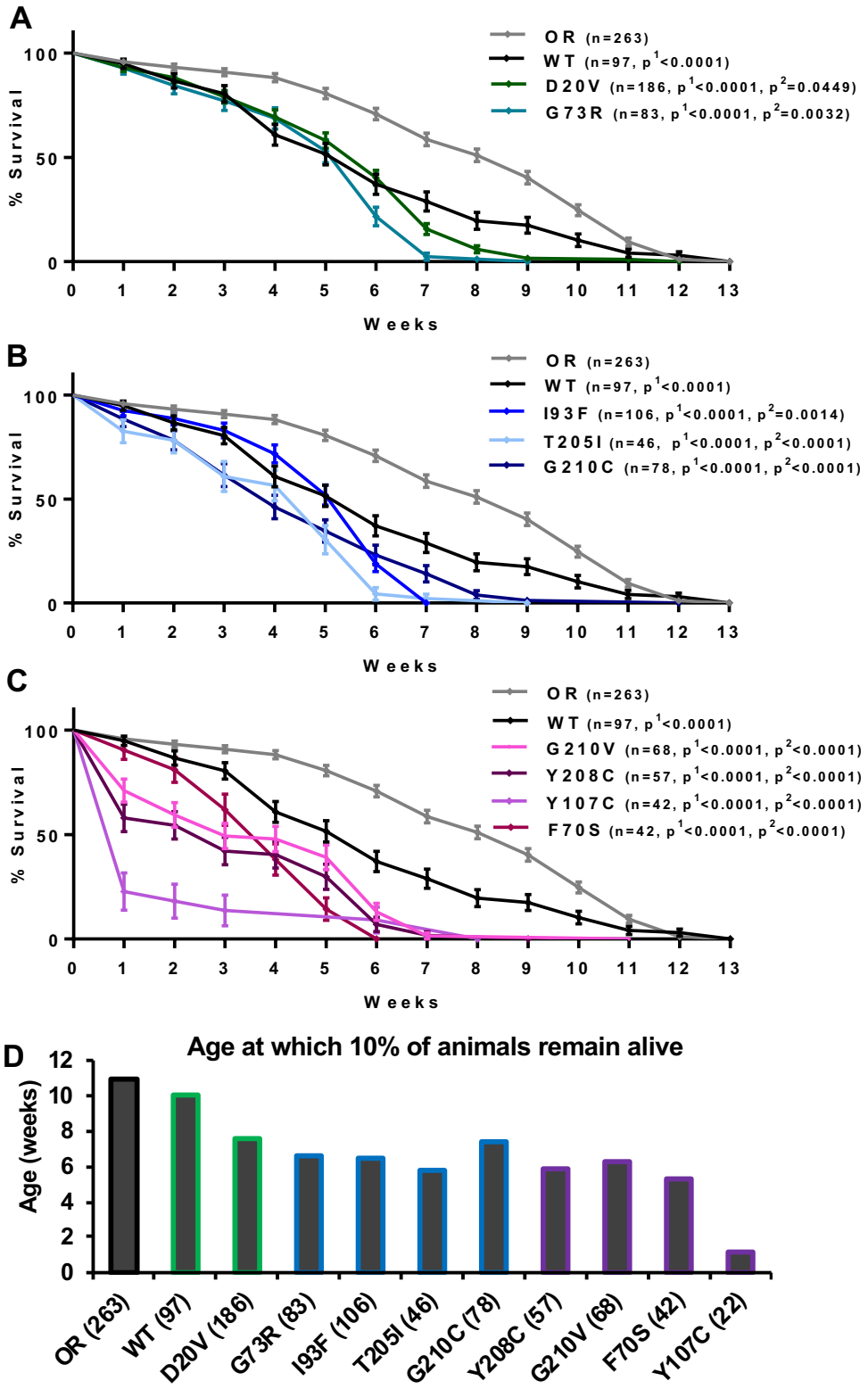

Figure 6. *Smn* missense mutations reduce lifespan A-C) Survival curves for adult flies expressing *Smn* missense mutations. Data is split into three graphs for visual clarity. Colors correspond to phenotypic Class. **D)** Lifespan measured as the age at which 10% of animals remain alive for each missense mutation. Shown next to genotypes, n-value (# of individual flies), p^1 (p-value as compared to OR, and p^2 (p-value as compared to WT). p-values were generate by Chi square analysis using the logrank rank/Mantel-Cox test.

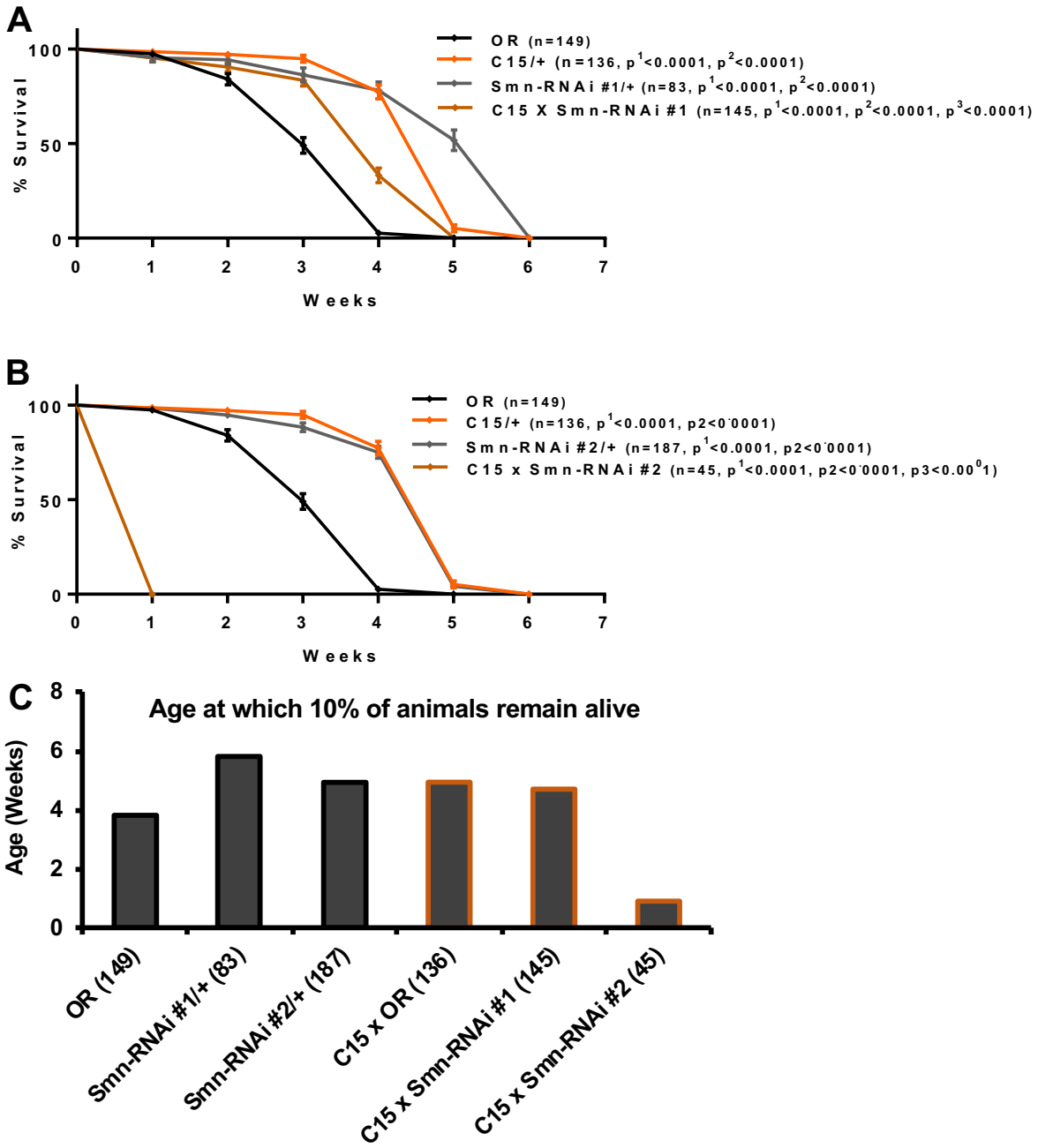

Figure 7. Neuromuscular *Smn* knockdown reduces lifespan. A and B) Survival curves for adult flies expressing Smn-RNAi in all neurons and muscles. **C)** Lifespan measured as the age at which 10% of animals remain alive for each missense mutation. Shown next to genotypes, n-value (# of individual flies), p^1 (p-value as compared to OR, p^2 (p-value as compared to C15 x OR), and p^3 (p-value as compared to the respective Smn-RNAi/+). p-values were generate by Chi square analysis using the logrank rank/Mantel-Cox test.

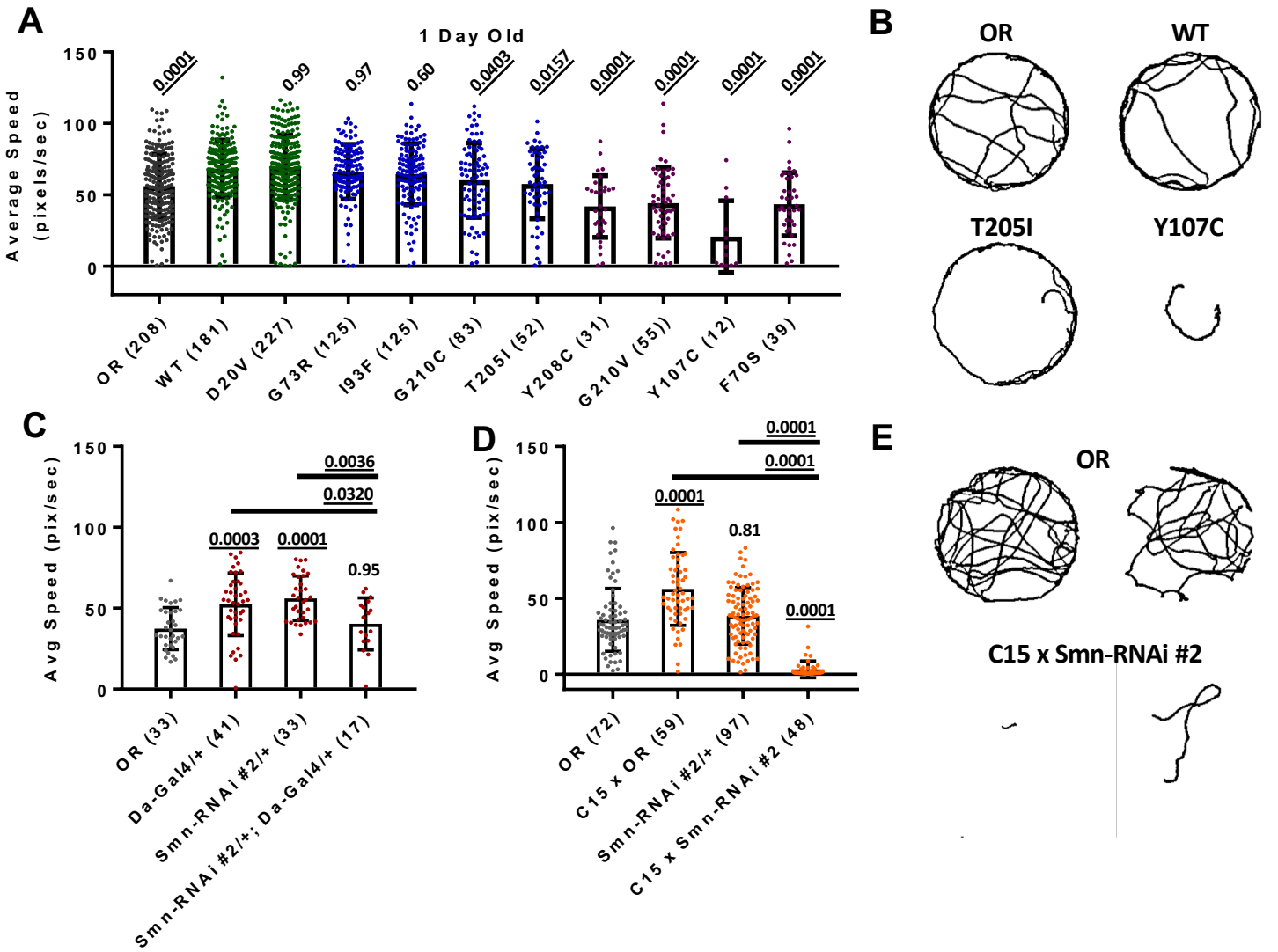

Figure 8. *Smn* missense mutations or knockdown reduces free moving adult locomotion. A) Adult walking speed, measured in pixels/second, in adults one day after eclosion for animals expressing *Smn* missense mutations . **B)** Representative traces for the data shown in A. **C and D)** Adult waking speed, measured in pixels per second, in adults one day after eclosion for animals expressing *Smn-RNAi* either ubiquitously with the Da-Gal4 driver (C) or in both neurons and muscle using the C15 driver line (D). **E)** Representative traces for the data shown in D. **Data:** Bars show average. Error bars show standard error. Data points and n-values (shown in parentheses next to genotypes) reflect the number of individual animals assayed. **Statistical analysis:** Values above the data are p-values vs WT from one-way ANOVA using the Dunnet correction for multiple comparisons. The p-values shown are multiplicity adjusted p-values. Underlining denotes values that are statistically significant.

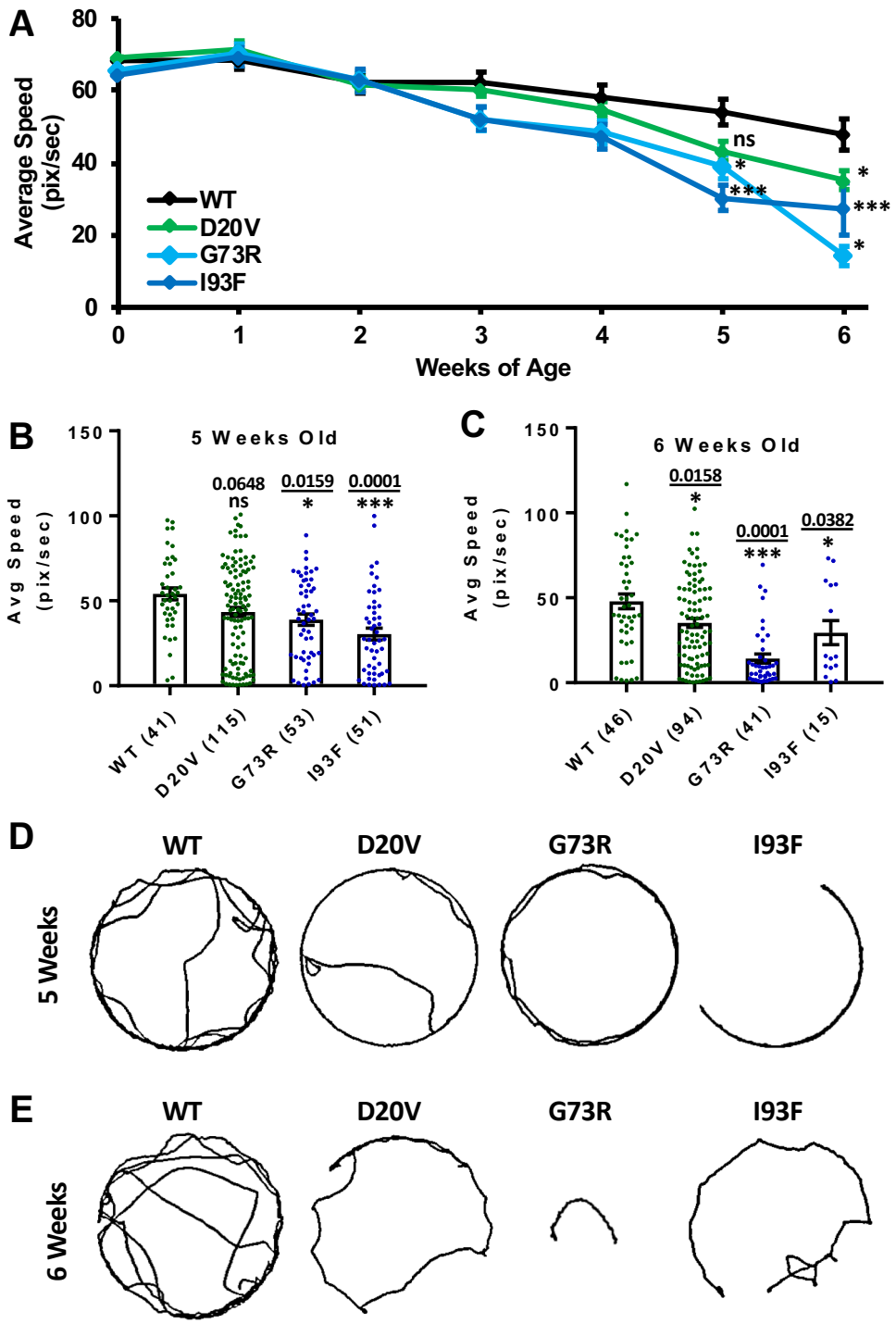

Figure 9. Animals expressing mild *Smn* missense mutations develop late-onset locomotor defects as adults. A) Adult walking speed, measured in pixels/second, in adults ranging from one day of age (0 weeks) through 6 weeks of age for animals expressing the WT transgene or the D20V, G73R, I93F *Smn* missense mutations. **B and C)** Adult walking speed (pixels/second) for the same genotypes shown in A at either 5 weeks or age (B) or 6 weeks of age (C). **D)** Representative traces for the data shown in B **E)** Representative traces for the data shown in C. **Data:** In A, points show averages in B and C, bars show average. Error bars show standard error in all cases. Data points and n-values (shown in parentheses next to genotypes) reflect the number of individual animals assayed. **Statistical analysis:** Values above the data are p-values vs WT from one-way ANOVA using the Dunnet correction for multiple comparisons. The p-values shown are multiplicity adjusted p-values. Underlining denotes values that are statistically significant. Stars shown in A correspond to exact p-values shown in B and C.

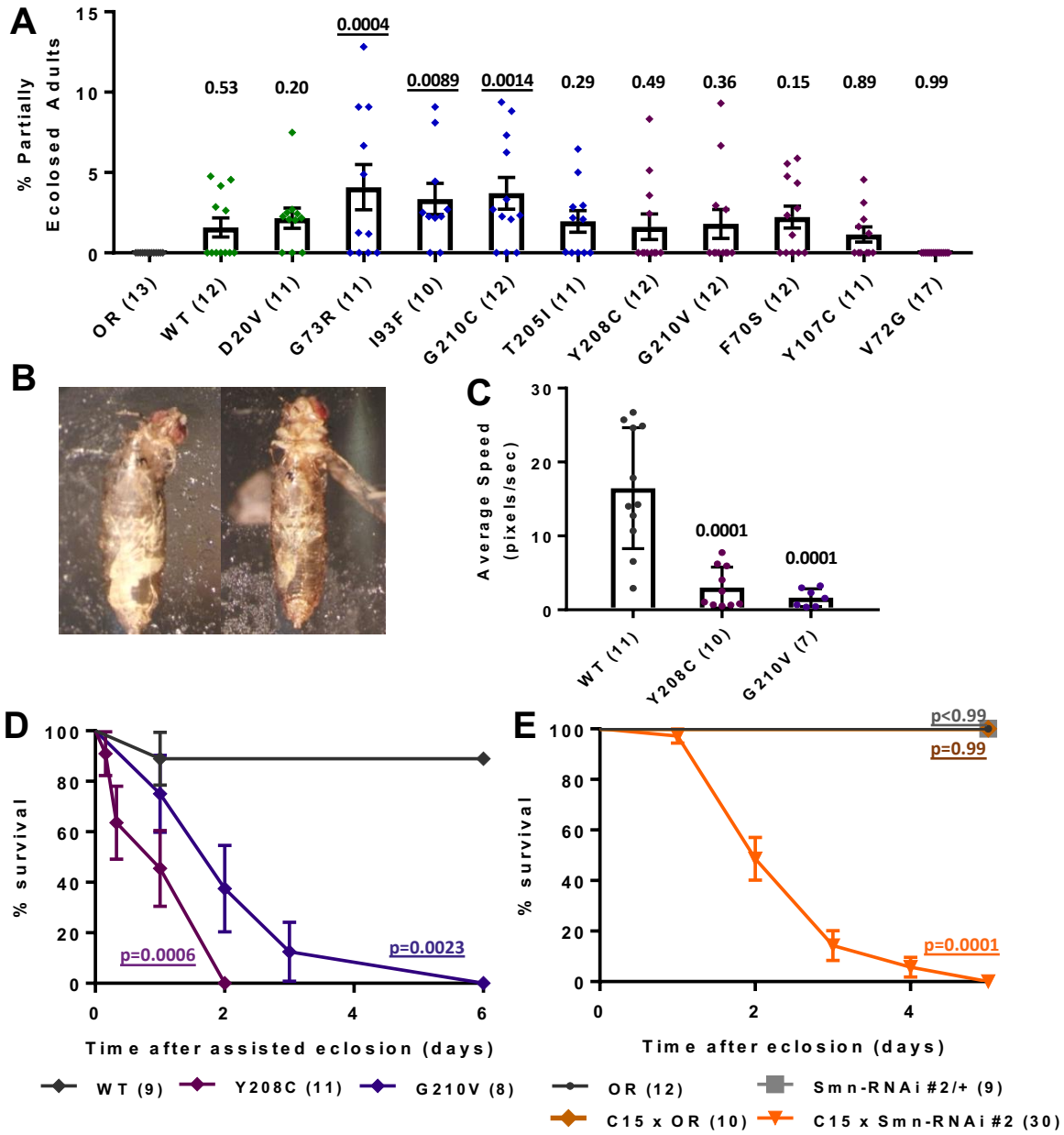

Figure 10. *Smn* missense mutants exhibit defect in eclosion. A) Percent of total larvae that complete pupal development but only partially eclose from their pupal case. **B)** Representative images of the partial eclosion phenotype quantified in A. **C)** Adult walking speed (pixels/second) for partially eclosed animals expressing the wild type *Smn* transgene or the Smn missense mutations Y208C or G210V. **D)** Survival curve for the same animals assayed in C. **E)** Survival curve for animals expressing neuromuscular *Smn* knockdown. **Data:** Bars show average. Error bars show standard error. Data points and n-values (shown in parentheses next to genotypes) reflect the number of individual animals assayed. **Statistical analysis:** For A and C, values above the data are p-values vs WT from one-way ANOVA using the Dunnet correction for multiple comparisons. The p-values shown are multiplicity adjusted p-values. Underlining denotes values that are statistically significant. For D and E, values next to each survival curve are p-values generated by Chi square analysis using the logrank rank/Mantel-Cox test.

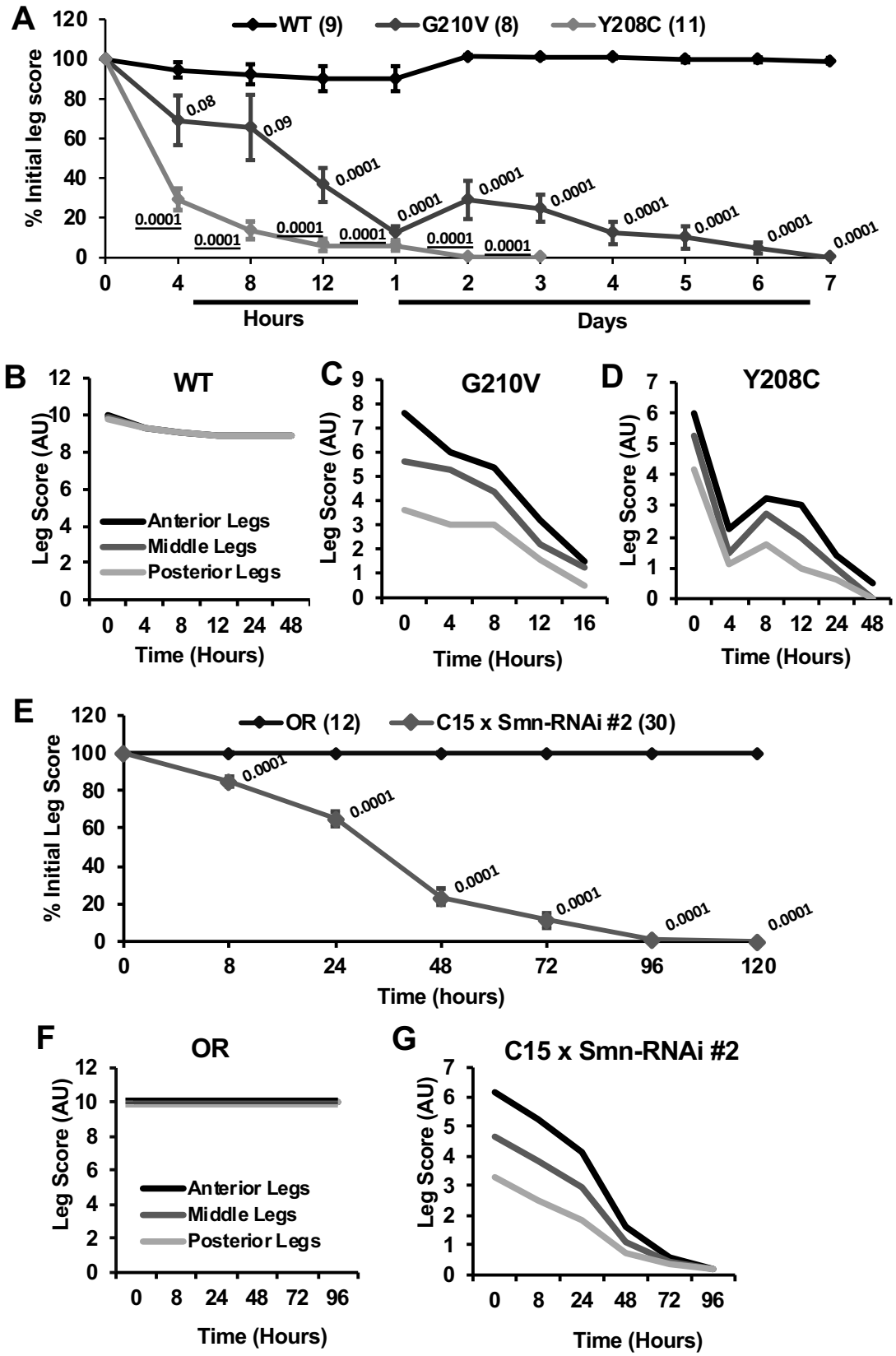

Figure 11. Progressive loss of motor function is observed in the legs of partially eclosed *Smn* missense mutants and in animals expressing neuromuscular Smn knockdown. A Qualitative leg function scores (average or all three leg pairs) over time for partially eclosed animals expressing the wild type *Smn* transgene (n=11) or the Y208C (n=10) or G210V (n=7) *Smn* missense mutations. **B-D)** Qualitative leg function scores for each leg pair over time for same animals as in A. **E)** Qualitative leg function scores (average or all three leg pairs) over time for animals expressing neuromusuclar *Smn* knockdown. **F and G)** Qualitative leg function scores for each leg pair over time for same animals as in E.

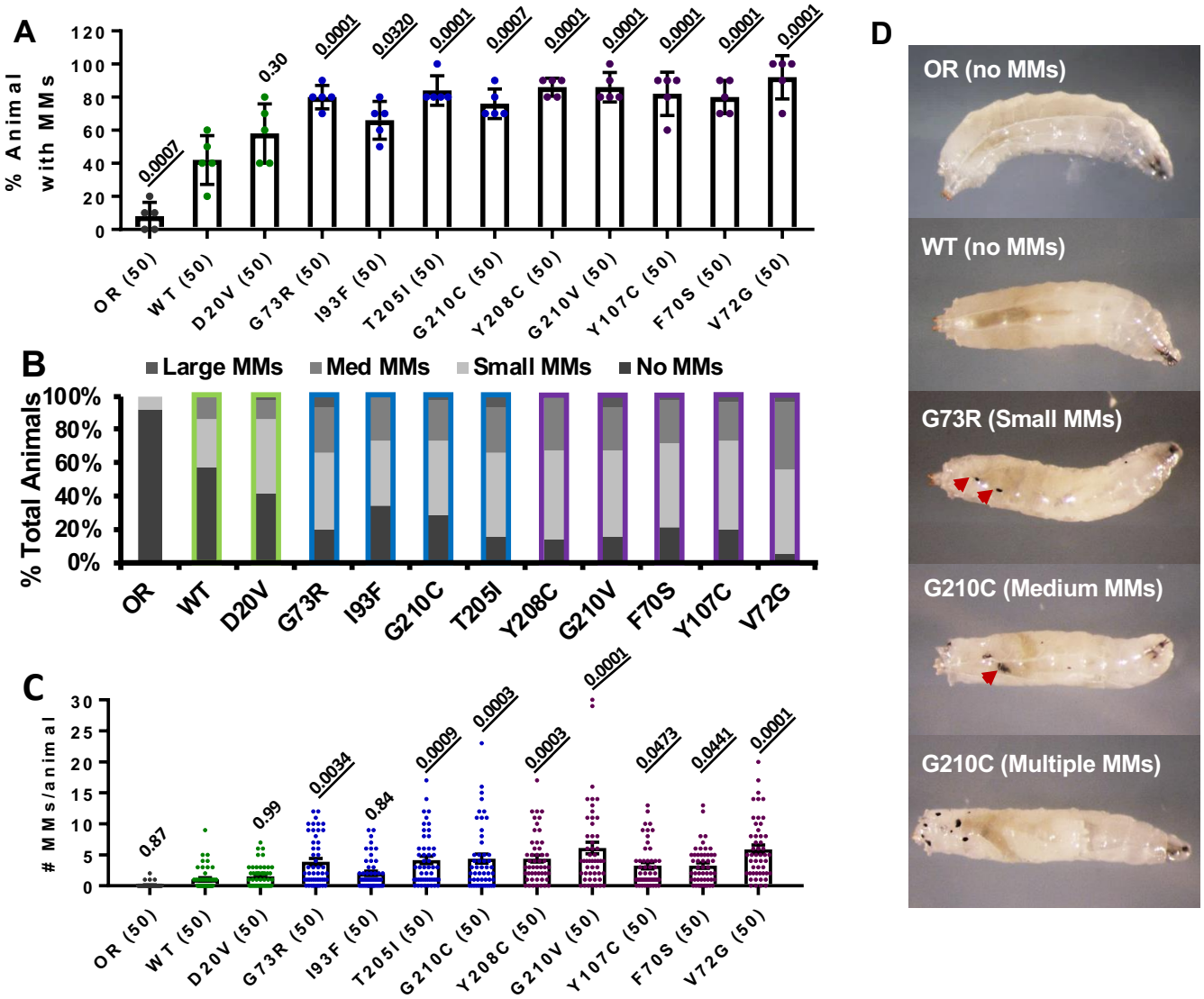

Figure 12. The innate immune system is activated in *Smn* missense mutants. A-C) Melanotic mass data for wandering third instar larvae expressing Smn missense mutations. The data in each panel a different measure of the melanotic mass phenotypes of the same set of larvae. **A)** Percent of larvae assayed that had one or more observable melanotic mass. **B)** Qualitative size scoring of the largest melanotic mass in each larvae. **C)** The average number of melanotic masses per animal. **D)** Representative images of melanotic masses in animals expressing *Smn* missense mutations. **Data:** Bars show average. Error bars show standard error. In A, data points represent biological replicates of 10 animals each and n-values (shown in parentheses next to genotpes) reflect the number of individual animas assyed. In C, data points and n-values reflect the number of individual animals assayed. **Statistical analysis:** Values above the data are p-values vs WT from one-way ANOVA using the Dunnet correction for multiple comparisons. The p-values shown are multiplicity adjusted p-values. Underlining denotes values that are statistically significant.

Figure Panel	Type of Data	Statistical Test	Correction for Multiple Comparison	F-value	p-value	R^2
1A	Normal	One-way Anova	Dunnet	F(16,120) = 24.22	0.0001	0.7635
1B	Normal	One-way Anova	Dunnet	F(16,120) = 131.7	0.0001	0.9461
1C - Early	Normal	One-way Anova	Dunnet	F(13,156) = 90.39	0.0001	0.8828
1C - Late	Normal	One-way Anova	Dunnet	F(13,156) = 32.61	0.0001	0.7321
1C - Adult	Normal	One-way Anova	Dunnet	F(13,156) = 308.6	0.0001	0.9628
2A	Normal	One-way Anova	Dunnet	F(7, 56) = 8.78	0.0001	0.5232
2B	Normal	One-way Anova	Dunnet	F(7, 56) = 48.93	0.0001	0.8595
3A	Normal	One-way Anova	Dunnet	F(17, 671) = 54.38	0.0001	0.5794
3C	Normal	One-way Anova	Dunnet	F(17, 671) = 44.24	0.00001	0.5303
3D	Normal	One-way Anova	Dunnet	F(13, 545) = 21.68	0.0001	0.3426
3F	Normal	One-way Anova	Dunnet	F(13, 545) = 3.545	0.0001	0.0780
4A	Normal	One-way Anova	Dunnet	F(14,195) = 2.369	0.0046	0.1454
4C	Normal	One-way Anova	Dunnet	F(14, 194) = 1.583	0.0865	0.1026
5A	Normal	One-way Anova	Dunnet	F(8, 55) = 16.31	0.0001	0.7035
5B	Normal	One-way Anova	Dunnet	F(8, 55) = 64.07	0.0001	0.9031
5C	Normal	One-way Anova	Dunnet	F(8, 179) = 14.03	0.0001	0.3853
6A	Survival data	Logrank/Mantel-Cox Test	Bonferroni	Corrected significance at p<0.0026		
6B	Survival data	Logrank/Mantel-Cox Test	Bonferroni	Corrected significance at p<0.0026		
6C	Survival data	Logrank/Mantel-Cox Test	Bonferroni	Corrected significance at p<0.0026		
7A	Survival data	Logrank/Mantel-Cox Test	Bonferroni	Corrected significance at p<0.0056		
7B	Survival data	Logrank/Mantel-Cox Test	Bonferroni	Corrected significance at p<0.0056		
8A	Normal	One-way Anova	Dunnet	F(11, 1242)= 21.36	0.0001	0.1591
8C	Normal	One-way Anova	Dunnet	F(5, 157) = 9.473	0.0001	0.2318
8D	Normal	One-way Anova	Dunnet	F(5, 404) = 52.56	0.0001	39.4100
9B	Normal	One-way Anova	Dunnet	F(3, 256) = 6.607	0.0003	0.0719
9C	Normal	One-way Anova	Dunnet	F(3, 192) = 13.39	0.0001	0.1730
10A	Normal	One-way Anova	Dunnet	F(13, 157)= 4.06	0.0001	0.2514
10C	Normal	One-way Anova	Dunnet	F(2, 25) = 22.01	0.0001	0.6378
10D	Survival data	Logrank/Mantel-Cox Test	Bonferroni	Corrected significance at p<0.025		
10E	Survival data	Logrank/Mantel-Cox Test	Bonferroni	Corrected significance at p<0.012		
11A - 4 hrs	Normal	One-way Anova	Dunnet	F(2, 70) = 29.71	0.0001	0.4591
11A - 8 hrs	Normal	One-way Anova	Dunnet	F(2, 67) = 45.55	0.0001	0.5762
11A -12 hrs	Normal	One-way Anova	Dunnet	F(2, 73) = 62.00	0.0001	0.6294
11A - 1 day	Normal	One-way Anova	Dunnet	F(2, 73) = 97.65	0.0001	0.7279
11A - 2 days	Normal	One-way Anova	Dunnet	F(2, 73) = 129	0.0001	0.7795
11A - 3 days	Normal	One-way Anova	Dunnet	F(2, 79) = 156.6	0.0001	0.7988
11A - 4 days	Normal	Student's T-test	N/A	F(23, 24) = 1.98	0.0001	0.7659
11A -5 days	Normal	Student's T-test	N/A	F(23, 24) = 1.96	0.0001	0.7679
11A - 6 days	Normal	Student's T-test	N/A	F(23, 24) = 1.99	0.0001	0.9233
11E - 8 hrs	Normal	Student's T-test	N/A	F(89, 35) = 1.99	0.0001	0.3959
11E - 24 hrs	Normal	Student's T-test	N/A	F(89, 35) = 1.99	0.0001	0.2085
11E - 48 hrs	Normal	Student's T-test	N/A	F(89, 35) = 1.99	0.0001	0.5020
11E - 72 hrs	Normal	Student's T-test	N/A	F(89, 35) = 1.99	0.0001	0.6336
11E - 96 hrs	Normal	Student's T-test	N/A	F(89, 35) = 1.99	0.0001	0.6336
12A	Normal	One-way Anova	Dunnet	F(13, 56) = 19.17	0.0001	0.8165
12C	Normal	One-way Anova	Dunnet	F(13, 686) = 12.9	0.0001	0.1964

Table 1. Information on all statistical analysis. Statistical analysis was performed using GraphPad Prism 7 and includes corrections for multiple comparisons when appropriate.

Human Mutation	Human Protein	Fly Protein	Protein Domain	# Patients Reported	Human SMA Type	SMN2 Copy #	Fly Phenotypic Class	Primary Reference
c.131A>T	D44V	D20V	Gemin2 binding	1	III	1	IV	Sun et al., 2005
c.275G>C	W92S	F70S	Tudor domain	2	I	3	II	Kotani et al., 2007
c.281T>G	V94G	V72G	Tudor domain	1	II	3	II	Clermont et al., 2004
c.283G>C	G95R	G73R	Tudor domain	1	III	1	III	Sun et al., 2005
c.346A>T	I116F	I93F	Tudor domain	1	I	1	III	Cusco et al., 2004
c.389A>G	Y130C	Y107C	Tudor domain	1	NR	NR	II	Prior, 2007
c.788T>G	M263R	M194R	YG box	1	I	2	I	Clermont et al., 2004
c.815A>G	Y272C	Y203C	YG box	11	I/II/III	1/2/3	I	Wirth et al., 1999
c.821C>T	T274I	T205I	YG box	4	II/III	1/2	III	Wirth et al., 1999
c.856G>C	G275S	G206S	YG box	1	III	NR	I	Skordis et al 2001
c.830A>G	Y277C	Y208C	YG box	1	II	1	II	Yamamoto et al. 2013
c.868G>T	G279C	G210C	YG box	2	II/III	NR	III	Wang et al., 1998
c.869G>T	G279V	G210V	YG box	2	I	NR	II	Talbot et al., 1997

Table 2. SMN missense mutation information from human patients and fly. When multiple SMA types and *SMN2* copy numbers are present, the order of the information for each criteria corresponds such that the first SMA type shown corresponds to the first *SMN2* copy number listed for a given mutation and so on and forth.

Human Protein	Fly Protein	SMN2 Copy #	SMA Type	Fly Phenotypic Class
D44V	D20V	1	III	IV
G95R	G73R	1	III	III
I116F	I93F	1	I	III
T274I	T205I	1/2	II/III	III
Y277C	Y208C	1	II	II
W92S	F70S	3	I	II
V94G	V72G	3	II	II
M263R	M194R	2	I	I
Y272C	Y203C	1/2/3	I/II/III	I

Table 3. Alignment of phenotypic severity between humans fly. *Smn* missense mutations are shown in order of least severe to most severe based on fly genotypes with the corresponding information from human patients. The four missense mutations with unknown *SMN2* copy number (Y107C, G206S, G210C, and G210V, shown in Table 1) have been excluded here to prevent potentially inaccurate comparisons.